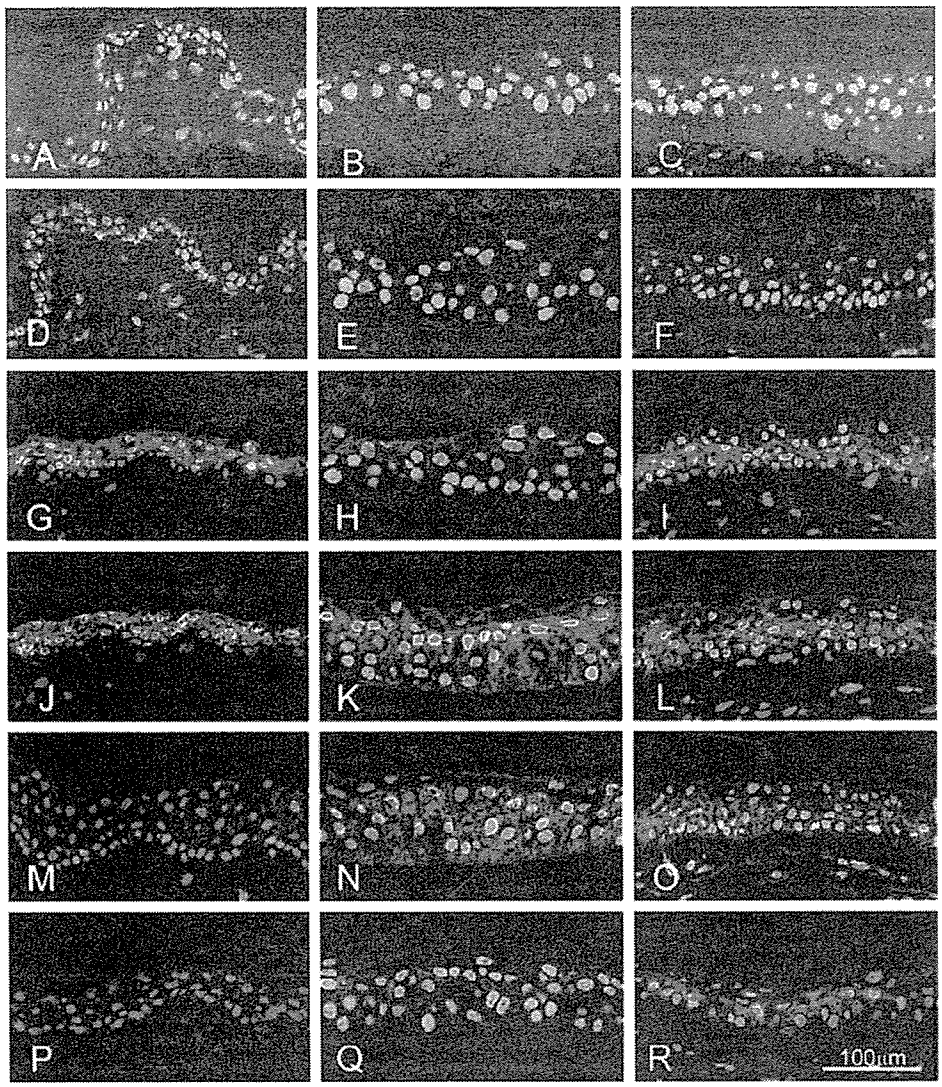

FIGURE 7. Immunohistochemical examination of the engrafted epithelium. In vivo HCjE (**A**, **D**, **G**, **J**, **M**, **P**), cultivated HCjE (**B**, **E**, **H**, **K**, **N**, **Q**), and engrafted epithelium (**C**, **F**, **I**, **L**, **O**, **R**) were immunostained (*green*) with MUC4 (**A**–**C**), MUC5AC (**D**–**F**), CK4 (**G**–**I**), CK13 (**J**–**L**), CK3 (**M**–**O**), or CK12 (**P**–**R**) and counterstained with propidium iodide (*red*).

ment. Because we were dealing with xenotransplantation, one of the limitations of this study is the short follow-up period of 14 days. With more prolonged follow-up, it may be that some conjunctival cells would differentiate into goblet cells and that progressive conjunctivalization and neovascularization would occur. More long-term studies are needed to investigate some of these questions.

In summary, ours is the first report that clearly demonstrates the potential of cultivated HCjE as an alternative tissue source for replacement of the corneal epithelium. Our animal study is a step toward the eventual transplantation of autologous cultivated HCjE to treat patients with ocular surface disorders, and studies are ongoing to resolve outstanding issues.

Acknowledgments

The authors thank John Bush and Christine Kime for reading the article and the Northwest Lion's EyeBank foundation for helping to obtain fresh human corneal tissues.

References

1. Kinoshita S, Friend J, Kiorpes TC, Thoft RA. Keratin-like proteins in corneal and conjunctival epithelium are different. *Invest Ophthalmol Vis Sci.* 1983;24:577–581.
2. Wei ZG, Sun TT, Lavker RM. Rabbit conjunctival and corneal epithelial cells belong to two separate lineages. *Invest Ophthalmol Vis Sci.* 1996;37:523–533.
3. Nishida K, Adachi W, Shimizu-Matsumoto A, et al. A gene expression profile of human corneal epithelium and the isolation of human keratin 12 cDNA. *Invest Ophthalmol Vis Sci.* 1996;37:1800–1809.
4. Dota A, Nishida K, Adachi W, et al. An expression profile of active genes in human conjunctival epithelium. *Exp Eye Res.* 2001;72:235–241.
5. Lemp MA, Holly FJ, Iwata S, Dohlman CH. The precorneal tear film. I Factors in spreading and maintaining a continuous tear film over the corneal surface. *Arch Ophthalmol.* 1970;83:89–94.
6. Gipson IK. Distribution of mucins at the ocular surface. *Exp Eye Res.* 2004;78:379–388.
7. Koizumi N, Inatomi T, Suzuki T, Sotozono C, Kinoshita S. Cultivated corneal epithelial stem cell transplantation in ocular surface disorders. *Ophthalmology.* 2001;108:1569–1574.
8. Tsai RJ, Li LM, Chen JK. Reconstruction of damaged corneas by transplantation of autologous limbal epithelial cells. *N Engl J Med.* 2000;343:86–93.
9. Schwab IR, Reyes M, Isseroff RR. Successful transplantation of bioengineered tissue replacements in patients with ocular surface disease. *Cornea.* 2000;19:421–426.
10. Ramaesh K, Dhillon B. Ex vivo expansion of corneal limbal epithelial/stem cells for corneal surface reconstruction. *Eur J Ophthalmol.* 2003;13:515–524.

11. Meller D, Pires RT, Tseng SC. Ex vivo preservation and expansion of human limbal epithelial stem cells on amniotic membrane cultures. *Br J Ophthalmol.* 2002;86:463–471.
12. Nakamura T, Inatomi T, Sotozono C, Koizumi N, Kinoshita S. Successful primary culture and autologous transplantation of corneal limbal epithelial cells from minimal biopsy for unilateral severe ocular surface disease. *Acta Ophthalmol Scand.* 2004;82:468–471.
13. Inatomi T, Nakamura T, Koizumi N, et al. Midterm results on ocular surface reconstruction using cultivated autologous oral mucosal epithelial transplantation. *Am J Ophthalmol.* 2006;141:267–275.
14. Nishida K, Yamato M, Hayashida Y, et al. Corneal reconstruction with tissue-engineered cell sheets composed of autologous oral mucosal epithelium. *N Engl J Med.* 2004;351:1187–1196.
15. Nakamura T, Inatomi T, Sotozono C, et al. Transplantation of cultivated autologous oral mucosal epithelial cells in patients with severe ocular surface disorders. *Br J Ophthalmol.* 2004;88:1280–1284.
16. Sangwan VS, Vemuganti GK, Iftekhar G, Bansal AK, Rao GN. Use of autologous cultured limbal and conjunctival epithelium in a patient with severe bilateral ocular surface disease induced by acid injury: a case report of unique application. *Cornea.* 2003;22:478–481.
17. Scuderi N, Alfano C, Paolini G, Marchese C, Scuderi G. Transplantation of autologous cultivated conjunctival epithelium for the restoration of defects in the ocular surface. *Scand J Plast Reconstr Surg Hand Surg.* 2002;36:340–348.
18. Ang LP, Tan DT, Cajucom-Uy H, Beuerman RW. Autologous cultivated conjunctival transplantation for pterygium surgery. *Am J Ophthalmol.* 2005;139:611–619.
19. Ang LP, Tan DT, Beuerman RW, Lavker RM. Development of a conjunctival epithelial equivalent with improved proliferative properties using a multistep serum-free culture system. *Invest Ophthalmol Vis Sci.* 2004;45:1789–1795.
20. Tan DT, Ang LP, Beuerman RW. Reconstruction of the ocular surface by transplantation of a serum-free derived cultivated conjunctival epithelial equivalent. *Transplantation.* 2004;77:1729–1734.
21. Koizumi N, Inatomi T, Quantock AJ, et al. Amniotic membrane as a substrate for cultivating limbal corneal epithelial cells for autologous transplantation in rabbits. *Cornea.* 2000;19:65–71.
22. Koizumi N, Cooper LJ, Fullwood NJ, et al. An evaluation of cultivated corneal limbal epithelial cells, using cell-suspension culture. *Invest Ophthalmol Vis Sci.* 2002;43:2114–2121.
23. Nishida K, Watanabe H, Ohashi Y, Kinoshita S, Manabe R. Effect of a new immunosuppressive agent, FK-506, on epithelial rejection after keratoepithelioplasty in rabbits. *Folia Ophthalmol Jpn.* 1991;42:851–856.
24. Yuge I, Takumi Y, Koyabu K, et al. Transplanted human amniotic epithelial cells express connexin 26 and Na-K-adenosine triphosphatase in the inner ear. *Transplantation.* 2004;77:1452–1454.
25. Zhang SC, Wernig M, Duncan ID, Brustle O, Thomson JA. In vitro differentiation of transplantable neural precursors from human embryonic stem cells. *Nat Biotechnol.* 2001;19:1129–1133.
26. Nakamura T, Kinoshita S. Ocular surface reconstruction using cultivated mucosal epithelial stem cells. *Cornea.* 2003;22:S75–S80.
27. Nakamura T, Endo K, Cooper LJ, et al. The successful culture and autologous transplantation of rabbit oral mucosal epithelial cells on amniotic membrane. *Invest Ophthalmol Vis Sci.* 2003;44:106–116.
28. Franke WW, Moll R, Mueller H, et al. Immunocytochemical identification of epithelium-derived human tumors with antibodies to desmosomal plaque proteins. *Proc Natl Acad Sci USA.* 1983;80:543–547.
29. Jones JC, Kurpakus MA, Cooper HM, Quaranta V. A function for the integrin alpha 6 beta 4 in the hemidesmosome. *Cell Regul.* 1991;2:427–438.
30. Rousselle P, Lunstrum GP, Keene DR, Burgeson RE. Kalinin: an epithelium-specific basement membrane adhesion molecule that is a component of anchoring filaments. *J Cell Biol.* 1991;114:567–576.
31. Kurpakus MA, Stock EL, Jones JC. The role of the basement membrane in differential expression of keratin proteins in epithelial cells. *Dev Biol.* 1992;150:243–255.
32. Pellegrini G, Dellambra E, Golisano O, et al. p63 identifies keratinocyte stem cells. *Proc Natl Acad Sci USA.* 2001;98:3156–3161.
33. Chen Z, de Paiva CS, Luo L, et al. Characterization of putative stem cell phenotype in human limbal epithelia. *Stem Cells.* 2004;22:355–366.
34. de Paiva CS, Chen Z, Corrales RM, Pflugfelder SC, Li DQ. ABCG2 transporter identifies a population of clonogenic human limbal epithelial cells. *Stem Cells.* 2005;23:63–73.
35. Inatomi T, Spurr-Michaud S, Tisdale AS, et al. Expression of secretory mucin genes by human conjunctival epithelia. *Invest Ophthalmol Vis Sci.* 1996;37:1684–1692.
36. Tei M, Spurr-Michaud SJ, Tisdale AS, Gipson IK. Vitamin A deficiency alters the expression of mucin genes by the rat ocular surface epithelium. *Invest Ophthalmol Vis Sci.* 2000;41:82–88.
37. Ellingham RB, Berry M, Stevenson D, Corfield AP. Secreted human conjunctival mucus contains MUC5AC glycoforms. *Glycobiology.* 1999;9:1181–1189.
38. McKenzie RW, Jumblatt JE, Jumblatt MM. Quantification of MUC2 and MUC5AC transcripts in human conjunctiva. *Invest Ophthalmol Vis Sci.* 2000;41:703–708.
39. Kessing SV. Investigations of the conjunctival mucin: quantitative studies of the goblet cells of conjunctiva—preliminary report. *Acta Ophthalmol (Copenh).* 1966;44:439–453.
40. Kawasaki S, Tanioka H, Yamasaki K, et al. Clusters of corneal epithelial cells reside ectopically in human conjunctival epithelium. *Invest Ophthalmol Vis Sci.* 2006;47:1359–1367.
41. Sekiyama E, Nakamura T, LJ. C, et al. Unique distribution of thrombospondin-1 in human ocular surface epithelium. *Invest Ophthalmol Vis Sci.* 2006;47:1352–1358
42. Pellegrini G, Traverso CE, Franzi AT, et al. Long-term restoration of damaged corneal surfaces with autologous cultivated corneal epithelium. *Lancet.* 1997;349:990–993.
43. Kenyon KR, Tseng SC. Limbal autograft transplantation for ocular surface disorders. *Ophthalmology.* 1989;96:709–722; discussion 722–703.

Ocular Surface Reconstruction With Combination of Cultivated Autologous Oral Mucosal Epithelial Transplantation and Penetrating Keratoplasty

TSUTOMU INATOMI, MD, PHD, TAKAHIRO NAKAMURA, MD, PHD, MINA KOJYO, MD, NORIKO KOIZUMI, MD, PHD, CHIE SOTOZONO, MD, PHD, AND SHIGERU KINOSHITA, MD, PHD

• PURPOSE: To report an assessment of the two-step surgical combination of cultivated autologous oral mucosal epithelial transplantation (COMET) and penetrating keratoplasty (PKP) used to treat patients with severe limbal deficiency disorders, and to investigate the keratin expression patterns of transplanted surviving oral mucosal epithelium.

• DESIGN: Observational case series.

• METHODS: Two patients with Stevens-Johnson syndrome and chemical eye injury were treated by COMET followed, approximately six months later, by a PKP triple procedure. In the course of a mean follow-up period of 22.5 months, their clinical outcomes and the efficacy of this two-step surgical procedure were assessed. In addition, the keratin expression in corneal buttons excised during PKP were immunohistochemically examined to characterize the oral mucosal epithelium that survived ectopically on the cornea. In vivo laser confocal microscopy was used to investigate the structure of the epithelium on the corneal grafts.

• RESULTS: The ocular surfaces were successfully reconstructed with cultivated autologous oral mucosal epithelial sheets and PKP. No clinical complications, such as persistent epithelial defects, rejections, or recurrence of cicatrization, were encountered. Postoperative best-corrected visual acuity was 20/125 in one patient and 20/100 in the other. The surviving oral mucosal epithelium, distinguished by its fluorescence pattern, consisted of an irregular, nonkeratinized, stratified epithelium without goblet cells. Immunohistochemical study demonstrated that K3, but not K12, was expressed in the transplanted cultivated oral mucosal epithelium that was similar to oral mucosal tissue. In vivo, the epithelial structure and cell density in the basal cell layer of the corneal grafts were similar to normal cornea.

• CONCLUSIONS: This study presents a two-step surgical approach to treat severely scarred ocular surfaces by means of a combination of COMET and PKP. Clinical outcomes suggest that this treatment may be beneficial for the maintenance of the reconstructed ocular surface by providing oral mucosal epithelium around the corneal graft. (Am J Ophthalmol 2006;142:757–764. © 2006 by Elsevier Inc. All rights reserved.)

Accepted for publication Jun 1, 2006.

From the Department of Ophthalmology, Kyoto Prefectural University of Medicine, Kyoto, Japan.

Supported in part by grants-in-aid for Translational Research and Scientific Research from the Japanese Ministry of Education, Culture, Sports, and Science and Technology (Kobe Translational Research Cluster); grants from the Japanese Ministry of Health, Labor, and Welfare (H16-Saisei-007); and a research grant from the Kyoto Foundation for the Promotion of Medical Science.

Inquiries to Tsutomu Inatomi, MD, PhD, Department of Ophthalmology, Kyoto Prefectural University of Medicine, Kawaramachi Hirokoji, Kamigyo-ku, Kyoto 602-0841, Japan; e-mail: tinatomi@ophth.kpu-m.ac.jp

BECAUSE SEVERE STEM CELL DEFICIENCY IS SOMETIMES accompanied by severe corneal stromal opacity and/or corneal endothelial dysfunction, most patients require penetrating keratoplasty (PKP) for visual rehabilitation. However, ocular surface reconstruction through corneal epithelial transplantation and PKP increases the risk for immunologic rejection and graft failure, and patients require long-term intensive immunosuppression and continuous care.[1,2]

Another clinical problem encountered in ocular surfaces reconstructed with PKP is the persistence of an epithelial defect after loss of the donor corneal epithelium. PKP without epithelial transplantation results in persistent epithelial defects as a result of the limited life span of the donor central corneal epithelium, especially in patients with limbal deficiency; the resultant graft-melting and conjunctival invasion severely compromises visual recovery. Therefore, to improve the clinical outcome and long-term

0002-9394/06/$32.00
doi:10.1016/j.ajo.2006.06.004

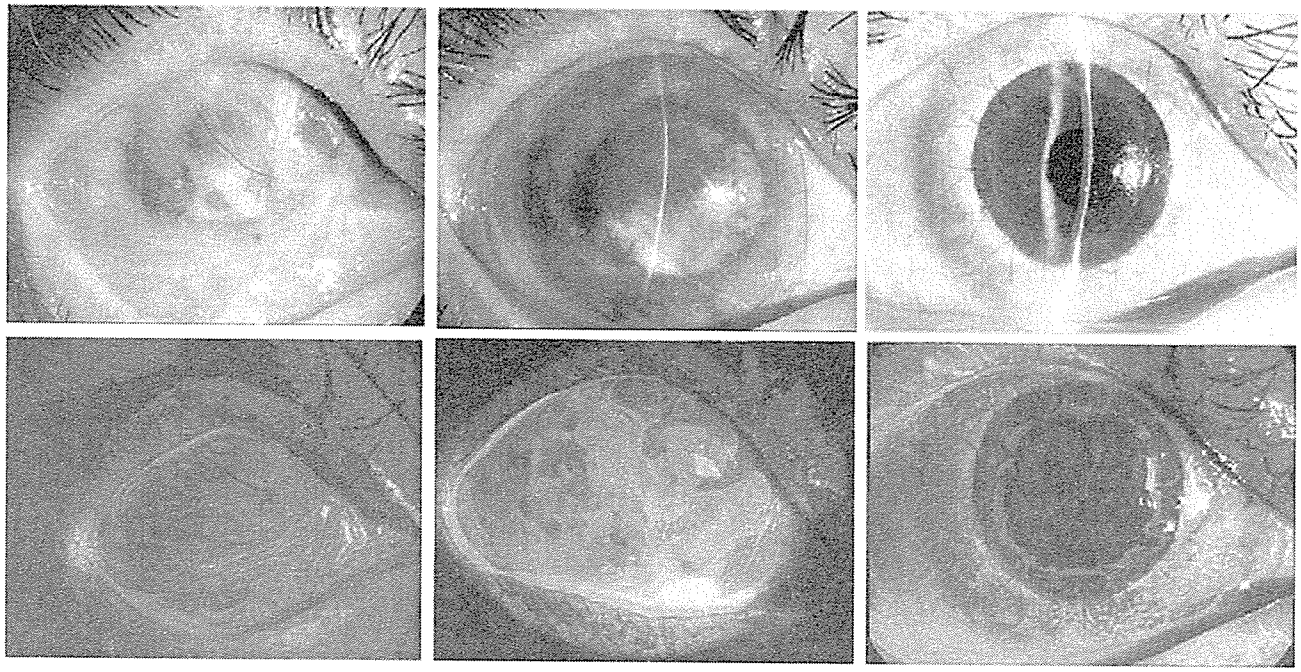

FIGURE 1. Clinical appearance before and after ocular surface reconstruction using cultivated autologous oral mucosal epithelial transplantation (COMET) and penetrating keratoplasty (PKP) in patient 1, a 70-year-old man with chemical injury. (Top left) Preoperatively, there is total conjunctivalization with severe scarring of both the cornea and conjunctiva. (Bottom left) Fluorescein staining. (Top center) Two months after initial surgery with COMET. (Bottom center) Uneven, hyperfluorescein staining pattern indicates survival of oral mucosal epithelium on ocular surface. (Top right) Status three months after PKP with cataract surgery. (Bottom right) Fluorescein staining demonstrated the slow invasion of oral mucosal epithelium surrounding the corneal graft.

prognosis of these patients, their reconstructed ocular surfaces must be provided with a more stable epithelial supply.

Pellegrini and associates[3] first reported the transplantation of cultivated corneal epithelium. Subsequent technical and surgical advances have made possible the grafting of cultivated corneal epithelial stem cell sheets.[4–8] Nakamura and associates[9] reported the successful transplantation of cultivated mucosal epithelial stem cell sheets derived from autologous cell sources. Autologous conjunctival epithelium[10,11] and nonocular (for example, oral mucosal) epithelium[12] have been used as a cell source for the cultivation of grafts to treat patients with bilateral ocular disorders. Because of its high proliferation potential, short cell-turnover time, and the safety of oral biopsy, oral mucosal epithelium has attracted attention as a cell source.[13,14] Initial clinical studies and midterm assessments of cultivated autologous oral mucosal epithelial transplantation (COMET) yielded favorable results from the perspective of ocular surface stabilization and visual recovery.[15–17] However, the cell biology and the longevity of surviving oral mucosal epithelium on the ocular surface require further investigation.

This study presents a two-step surgical strategy that uses a combination of COMET and PKP. The ocular surface was stable and the cornea remained transparent after the transplantation of cultivated oral mucosal epithelium when this two-step process is used. This surgical strategy reconstructs the ocular surface by transplanting a corneal graft that is surrounded by ectopically transplanted autologous oral mucosal epithelium just after the second PKP surgery, and the ectopically transplanted autologous oral mucosal epithelium may gradually cover the graft surface. This offers the potential for supplying mucosal epithelium for prolonged periods, and this high proliferation potential could possibly address the issue of wound healing. There is no direct evidence to date that oral mucosal epithelium would display a higher level of proliferation than ocular surface epithelium, but previous studies have demonstrated that oral mucosal epithelium has a high proliferation potential compared with epidermal cells.[13,14] On the basis of the condition of the oral mucosal epithelium, it is worth noting that this surgical concept and modality appear to have improved the clinical outcome of ocular surface disease that previously had a poor prognosis, although the follow-up period after PKP is relatively short.

METHODS

THIS STUDY WAS APPROVED BY THE INSTITUTIONAL REview Board for Human Studies of Kyoto Prefectural University of Medicine, and prior informed consent was obtained from all patients in accordance with the tenets of

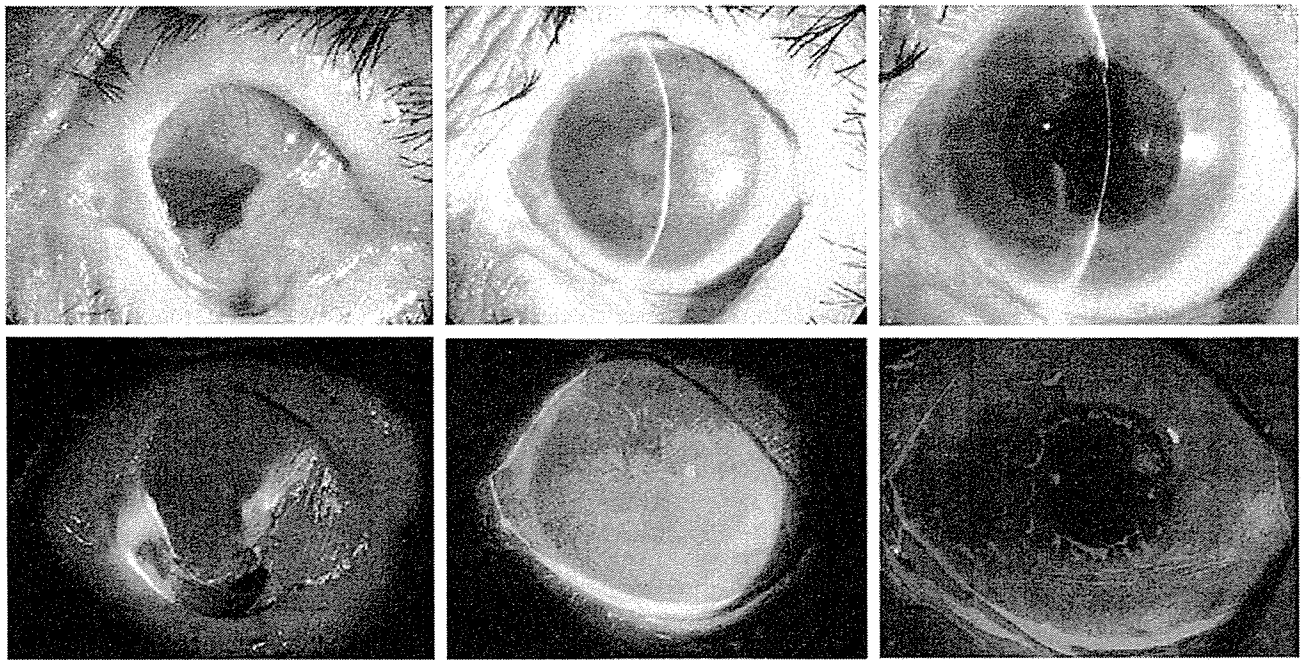

FIGURE 2. Clinical appearance before and after reconstruction using cultivated autologous oral mucosal epithelial transplantation (COMET) and penetrating keratoplasty (PKP) in patient 2, a 71-year-old man with Stevens-Johnson syndrome. (Top left) Preoperative total conjunctivalization with severe symblepharon and partial parakeratinization. (Bottom left) Fluorescein staining. (Top center) Two months after the initial surgery with COMET. (Bottom center) Fluorescein staining of surviving oral mucosal epithelium distinguishes between corneal and conjunctival epithelium. (Top right) Three months after PKP with cataract surgery. (Bottom right) Fluorescein staining demonstrated the presence of thicker oral mucosal epithelium surrounding the corneal graft.

the Declaration of Helsinki for research involving human subjects. This study involved two patients with bilateral total limbal deficiency; their ages were 70 and 71 years, respectively. The primary reason for their limbal deficiency and cicatrization was severe chemical injury and Stevens-Johnson syndrome. Both patients manifested severe destruction of the ocular surface; limbal deficiency was unequivocally diagnosed on the basis of the total replacement by scarred conjunctival tissue and the complete absence of the palisades of Vogt (Figures 1 and 2). Minimum reflex tearing was noted by slit-lamp examination and the Schirmer test, and there was sufficient meniscus height to maintain a wet mucous surface. Both patients presented severe scarring involving the full thickness of the cornea and restricted visibility of anterior chamber components. Patients 1 and 2 were followed for 26 and 19 months, respectively.

Human amniotic membrane (AM) was harvested at the time of elective caesarean section; preservation was at −80°C. Under sterile conditions, the membranes were deprived of their amniotic epithelium by two hours' incubation at 37°C with ethylenediamine tetraacetic acid (EDTA) 0.02% solution to loosen cell adhesion. This was followed by gentle scraping with a cell scraper.

The procedure for generating cultivated oral mucosal epithelial sheets has been reported by Nakamura and associates.[12,15] Under local anesthesia, 3 to 5 mm^2 oral mucosal biopsy specimens were obtained after proper treatment of the oral cavity. After removing submucosal connective tissues, small explants were immersed in phosphate-buffered (PBS) saline solution containing antibiotics (50 IU/ml penicillin-streptomycin and 5 μg/ml amphotericin B), incubated at 37°C for one hour with 1.2 IU dispase, and then treated with trypsin-EDTA 0.05% solution for 10 minutes at room temperature (RT) to separate the cells. The oral mucosal epithelium was then placed on denuded AM spread on the bottom of culture inserts and cocultured with mitomycin C–inactivated 3T3 fibroblasts. The culture was submerged in medium until cell confluence and then exposed to air by lowering the level of the medium for one to two days to promote epithelial differentiation. Cultures were incubated at 37°C in a 5% CO_2–95% air incubator; the medium was changed daily.

The initial surgical procedure for ocular surface reconstruction was as described in previous reports.[5,15] In brief, after a 360-degree conjunctival peritomy, conjunctivalized tissue on the corneal surface and thick, fibrotic subconjunctival tissues were removed. The subconjunctival spaces were treated with mitomycin C 0.04% for five minutes and then vigorously washed with saline solution. Then AM transplantation was carried out to reconstruct the conjunctival fornix. The preserved AM was placed with epithelial side up and then sutured with 10-0 nylon. After excising the AM covering the corneal surface, a

19-mm–diameter piece of cultivated autologous oral mucosal epithelial sheet was transplanted onto the corneal surface and sutured with 10-0 nylon. The integrity of the cultivated epithelium was confirmed by fluorescein staining at the end of surgery. Postoperatively, the transplanted epithelial sheet was protected with a medical-use contact lens.

PKP was performed five to six months after the initial COMET ocular surface reconstruction. PKP with cataract surgery was performed according to the usual procedures. In brief, a 7-mm–diameter trephination was performed on the host cornea, followed by continuous circular capsulorrhexis. The lens was removed by the regular phaco amelification and aspiration technique through the trephinated cornea. After inserting the intraocular lens, a 7.25-mm–diameter fresh donor cornea with epithelium was fastened with interrupted and continuous sutures. The corneal surface was then covered with a soft contact lens that was changed as appropriate during the follow-up period.

Immunohistochemical studies of keratin expression in the reconstructed ocular surface epithelium derived from cultivated oral mucosal epithelium were performed by using the previously described procedure.[12] Corneal buttons excised with a 7-mm–diameter trephine were examined at the time of the second surgery. Normal oral tissue was the control for immunohistochemical comparison studies; all tissues were stored at −80°C. Cryostat sections (7 μm in thickness) were placed on gelatin-coated slides, air dried, and rehydrated in PBS for 15 minutes at RT. The tissues were then incubated for 30 minutes at RT with bovine serum albumin 1% to block nonspecific bindings and further incubated (one hour, RT) with primary antibodies. Mouse monoclonal antibodies were used against keratin 1/10/4/13 (Novocastra, Newcastle, United Kingdom), keratin 3 (Progen, Heidelberg, Germany), and rabbit polyclonal antibodies against keratin 12 (Transgenic, Kumamoto, Japan). Control incubations were with appropriate normal mouse and rabbit IgG (Dako, Kyoto, Japan) at the same concentration as the primary antibody. After staining with the primary antibody, sections were incubated (one hour, RT) with the appropriate secondary antibodies; we used fluorescein isothiocyanate–conjugated donkey anti-mouse IgG (Jackson ImmunoResearch, West Grove, Pennsylvania, USA) and fluorescein isothiocyanate–conjugated donkey anti-rabbit IgG (Vector Laboratories, Burlingame, California, USA). After several washes with PBS, the sections were coverslipped with antifading mounting medium containing propidium iodide (Vectashield; Vector Laboratories) and examined under a confocal microscope (Fluoview; Olympus, Tokyo, Japan).

After more than one year of regular follow-up, an in vivo laser confocal microscope (Heidelberg Retinal Tomograph II/Rostock cornea module [HRT II]; Heidelberg Engineering, Heidelberg, Germany) was used for in vivo morphologic study of the reconstructed corneal epithelium on the corneal graft.[18] Confocal images in central regions were scanned from the apical layer to the basal epithelium. The density of the in vivo epithelium was measured by a computerized analysis system provided with the HRT II instrument.

RESULTS

ORAL MUCOSAL TISSUES WERE SAFELY EXCISED WITHOUT any complications. Approximately 1×10^5 oral mucosal epithelial cells were seeded onto the denuded AM and cultured for five to eight days until they reached confluence covering the entire AM. By two-week cultivation and air lifting, mature oral mucosal epithelium sheets that consisted of 5 to 6 cell layers were generated. Histologic examination confirmed that the sheets were comprised of well-differentiated stratified epithelium similar to that of the in vivo cornea; they consisted of a basal layer formed by cuboidal cells, several suprabasal cell layers, and flat apical cell layers. The condition of the cultivated epithelial sheet was confirmed by fluorescein staining at the end of the transplantation procedure. Both cases showed that the cultivated epithelial sheets were well stratified and without epithelial defect or any remarkable surface damage.

Patient 1 was a 70-year-old man who had experienced alkali burns to both eyes when he was 30 years old. Although history of previous surgeries was unavailable, slit-lamp examination showed round scarring in the peripheral cornea suggestive of earlier PKP. His right eye, chosen for ocular surface reconstruction, showed complete conjunctivalization on the corneal surface with extensive scarring and symblepharon formations (Figure 1). The intraocular status was unascertainable, yet ultrasound examination returned no abnormal vitreoretinal findings. His best-corrected visual acuity (BCVA) of the right eye was hand motion. On October 17, 2003, he underwent COMET and AM transplantation after the removal of scar tissue from both the cornea and subconjunctival space. Survival of the entire oral mucosal epithelium was confirmed on the second postoperative day, and it gradually covered the entire ocular surface. His visual acuity remained unchanged after the initial surgery. After the initial surgery, the reconstructed ocular surface showed uneven and irregular fluorescein staining absent of any epithelial defects (Figure 1). He experienced no recurrence of cicatrization or prolonged inflammation after the first operation. It is notable that the ocular surface before PKP was stable and uniform without inflammation. Because intraoperative observation showed the existence of a previous small PKP, PKP was selected to remove the corneal scar rather than lamellar keratoplasty. The second step, PKP combined with cataract surgery, was performed six months after the initial surgery; the graft had remained clear without any epithelial defect or rejection. There was minimal neovascularization along the sutures, but not in the corneal graft. A slow ingrowth of trans-

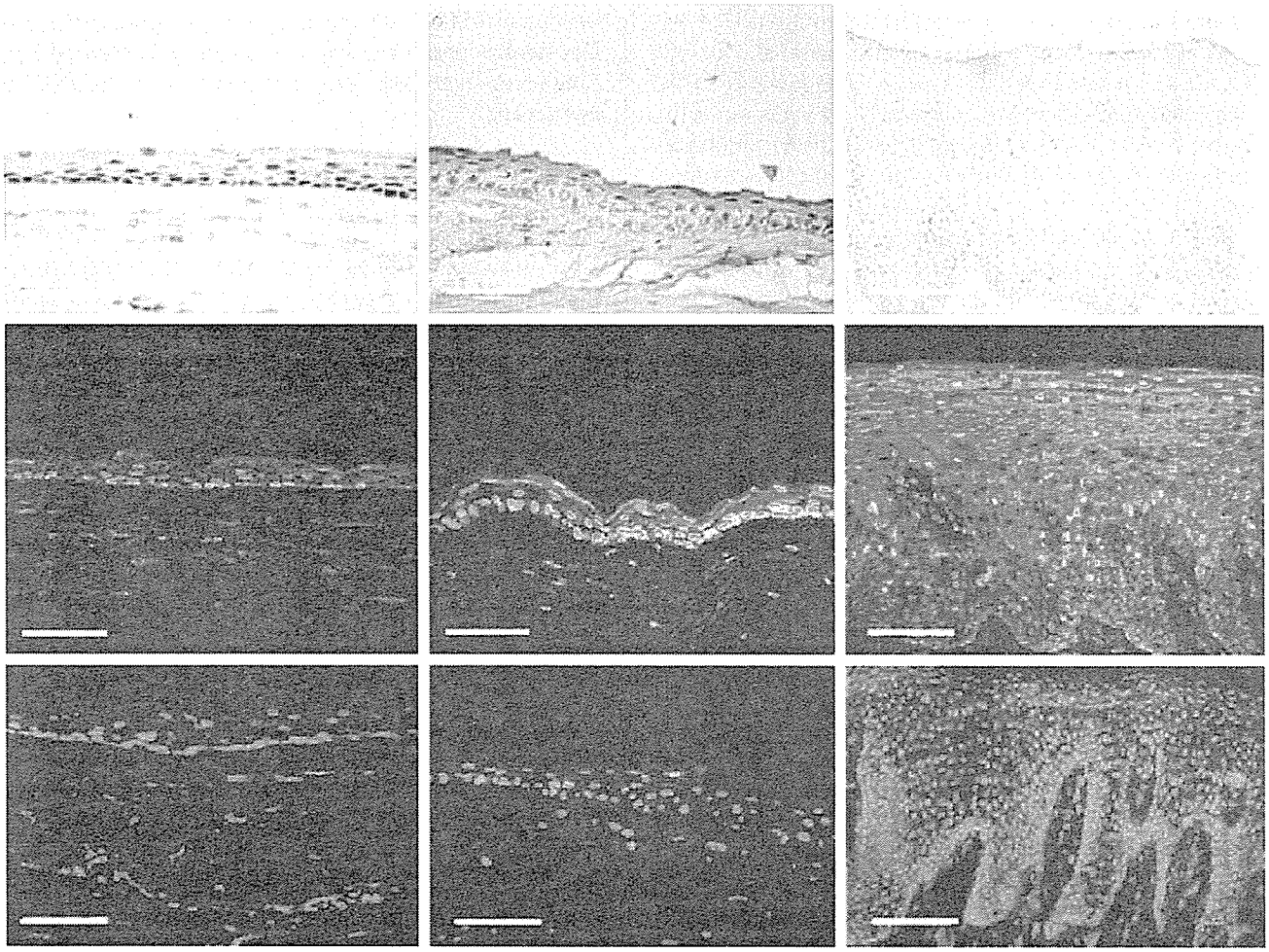

FIGURE 3. Immunohistological appearance of keratin 3 and 12 expressions in a cultivated oral mucosal epithelium sheet, surviving cultivated oral mucosal epithelium on the corneal button (subsequently resected at the time of penetrating keratoplasty [PKP]), and normal oral mucosal tissue. (Top left) Hematoxylin and eosin staining of a cultivated oral mucosal epithelial sheet from patient 1. (Second row, left) K3 expression in excised corneal button from patient 1. (Bottom left) There is no K12 expression in the excised corneal button from patient 1. (Top middle) Hematoxylin and eosin staining of cultivated oral mucosal epithelial sheet from patient 2. (Middle row, middle) K3 expression in excised corneal button from patient 2. (Bottom middle) K12 expression in excised corneal button from patient 2. (Top right) Hematoxylin and eosin staining of normal oral mucosal epithelium. (Middle row, right) K3 expression in normal oral mucosal epithelium. (Bottom right) Normal oral mucosal epithelium does not express K12. (Left and middle) Scale bars = 100 μm. (Right) Scale bar = 200 μm.

planted oral epithelium from the limbus was observed in the course of long-term follow-up (Figure 1). His BCVA improved to 20/100 and remained stable without reduction. Although his intraocular pressure (IOP) was occasionally high, he did not require glaucoma surgery. The occasional increase in IOP was managed by the topical application of carteolol hydrochloride 0.02% twice daily and latanoprost 0.05% once daily. Carbonic anhydrase inhibitor was also used to reduce IOP if the topical medication was not enough; however, no glaucoma surgery was required to control IOP.

Patient 2 was a 71-year-old man with no history of previous surgical treatment who had acquired Stevens-Johnson syndrome in his 40s. As shown in Figure 2, this patient had total conjunctivalization and severe scarring. He manifested minimal tear secretion and partial parakeratinization. Preoperatively, his visual acuity was hand movement. COMET was performed on this patient on May 26, 2004. There was an early epithelial defect in the center region during the two weeks after surgery; however, it healed without corneal melting or conjunctival invasion. His visual acuity remained unchanged after the initial operation. The second step, PKP with cataract surgery but not lamellar keratoplasty, was performed 5.5 months later by means of the standard procedure from the point of early visual rehabilitation. Subsequently, his BCVA improved to 20/125. He developed no postoperative complications except for a total corneal epithelial defect that originated

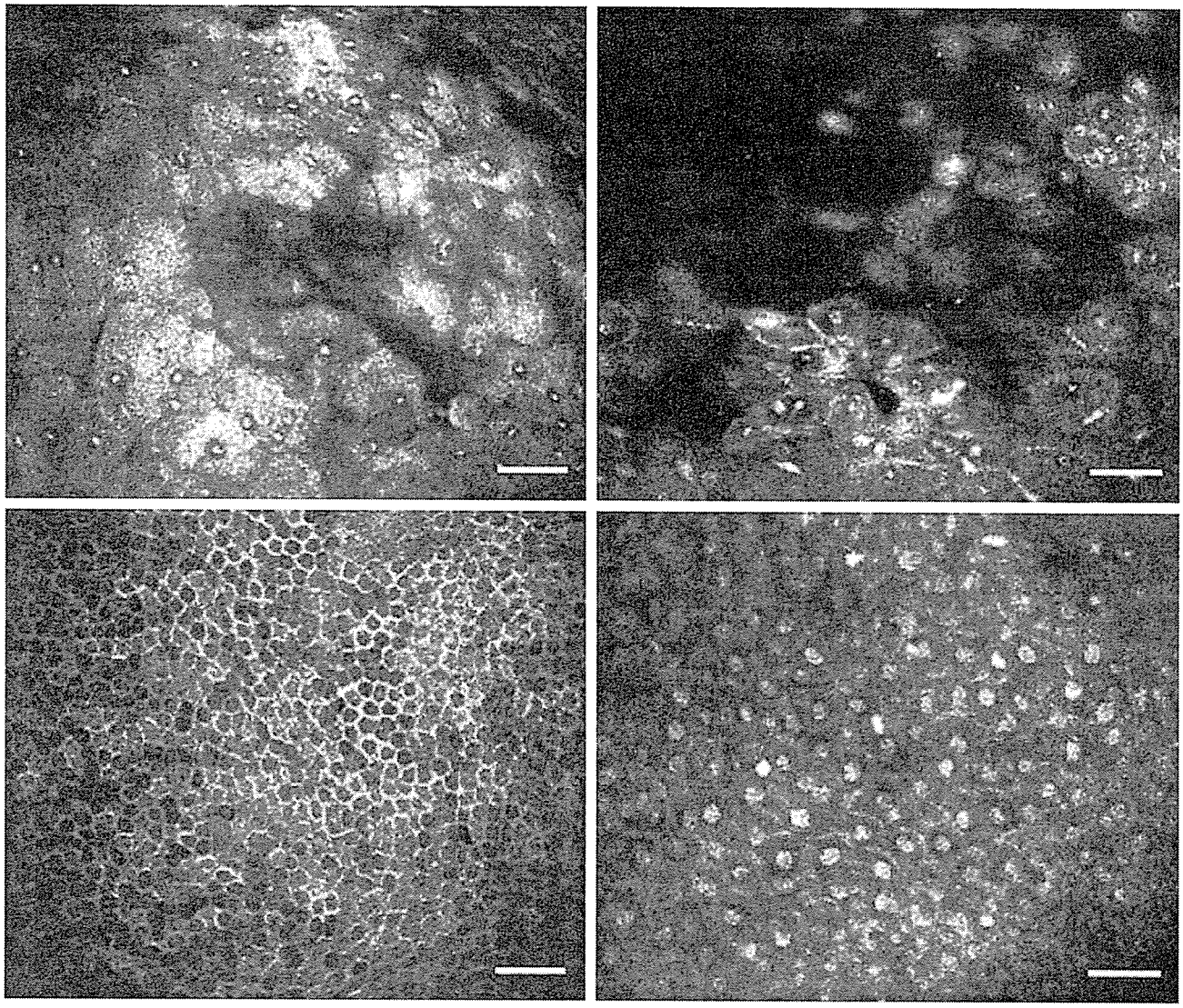

FIGURE 4. In vivo confocal micrographs demonstrate the appearance of the epithelium in the region of the transplanted central corneal surface. (Top left) Apical surface in patient 1. (Top right) Apical surface in patient 2. (Bottom left) Basal cell layers in patient 1. (Bottom right) Basal cell layers in patient 2. Note that the cell shape and density in each region are similar to normal cornea. Scale bars = 50 μm.

in the donor cornea after the medical contact lens fell off. However, the defect was gradually reepithelialized from the surrounding oral mucosal epithelium after rewear of the medical contact lens.

Immunohistochemical analysis was performed on the surviving transplanted cultivated oral mucosal epithelium on the cornea excised during PKP (Figure 3). Both patients demonstrated nonkeratinized stratified epithelium on the AM covering the cornea. Notably, in different regions, the stratified epithelium consisted of three to 10 layers; this finding was consistent with the results of slit-lamp examination. None of the specimens contained goblet cells. Immunohistochemistry confirmed the presence of K4 and K13; these keratins are specific for mucosal epithelium (data not shown). The expression of K1, which is specific for keratinized epithelium, was not detected (data not shown). As expected, K3 was expressed in surviving epithelium on the cornea as well as in oral mucosal epithelium. Conversely, K12, which is specific for corneal epithelium, was not expressed in the surviving epithelium, except for faint, occasional staining in the apical region.

We used the HRT II instrument for in vivo laser confocal scanning to study the histologic structure of the transplanted epithelium (Figure 4). The presence of a large, flat epithelium with small cell nuclei in the apical surface was noted in both patients; this is consistent with the normal corneal surface. The average cell density in the apical layer of the corneal graft was 840 ± 295 cells/mm^2 (mean ± SD) and not markedly different from a normal cornea.[18] The basal cells were smaller, denser, and aligned

in regular fashion, this also is similar to the normal corneal structure. The density of basal cells in the two patients was 8075.3 and 1492.0 cells/mm^2, respectively; in patient 1 it was within the range reported for normal central cornea (8996 ± 1532 cells/mm^2), whereas in patient 2 it was below the normal range.[18]

DISCUSSION

THIS STUDY PRESENTS A TWO-STEP SURGICAL APPROACH to treat patients with severe limbal deficiency disorder and corneal opacity. It consists of a combination of COMET and the conventional PKP triple-procedure. The two patients were followed for a mean of 22 months and encountered no immunologic rejection or persistent epithelial defect, common critical complications after combined surgical treatment consisting of corneal epithelial transplantation and PKP.

Cultivated autologous corneal epithelial transplantation that used AM was first introduced by Tsai and associates[4] and Koizumi and associates.[5] This tissue-engineered procedure promotes a strategy for reconstructing the corneal surface with autologous oral mucosal epithelium. This histologic study of the central cornea of two patients documents that transplanted cultivated oral mucosal epithelium on the corneal surface remained intact for at least the first six months after transplantation. Immunohistochemically, the surviving transplanted cultivated oral mucosal epithelium on the cornea was positive for K3 and K4 (data not shown) and negative for K10 (data not shown) and K12, indicating that it was neither corneal nor conjunctival. Rather, it resembled cultivated oral mucosal epithelium grown on AM. Thus, the intrinsic characteristics of the ectopically transplanted epithelium did not change. This finding coincides with observations made when cultivated oral mucosal epithelial sheets were transplanted onto rabbit eyes.[12] Because epithelial differentiation largely depends on the substrate, transplanted cultivated oral mucosal epithelial sheets do not resemble the in vivo oral mucosal epithelium, probably because of modifications induced by the external environment—that is, the corneal stroma or AM. The absence of neovascularization into the cornea after the grafting of oral mucosal epithelium may also be attributable to interaction with the corneal stroma. Studies are currently underway to elucidate biologic factors, such as mucin expression by surviving oral epithelium, to gain an understanding from the perspective of corneal function.

To improve the success rate of ocular surface reconstruction with PKP, allogenic recognition by the host immune system must be minimized. Therefore, limbal transplantation was avoided and a two-step approach was used instead. Tsubota and associates[19] demonstrated better graft survival when a two-step procedure was used to treat severe ocular surface disorders. The survival rate of limbal transplants and PKP grafts after combined surgery is relatively poor.[1,2,19] Because the limbal region contains allogenic antigens such as antigen-presenting cells and major histocompatibility complex class 2 molecules, allogenic limbal transplantation may be inappropriate in patients with severe limbal deficiency disorders. Although the findings of this study must be considered preliminary, they suggest that the mucosal epithelium covering the cornea, because it was derived from autologous oral mucosal epithelium, is not subject to allosensitization. Therefore, the results of this study indicate that this two-step procedure involves a risk for endothelial rejection that is no greater than that encountered with conventional PKP.

This two-step procedure features another improvement: the continuous, prolonged supply of epithelium, which compensates for the limited survival of corneal epithelium on the central corneal graft. However, although no epithelial defect was observed during the 22-month follow-up period, additional long-term observations are necessary to determine whether oral mucosal epithelial cells will offer continuous replacement on the transplanted cornea. Patients with limbal stem cell–deficient eyes often manifest persistent epithelial defects on their grafts after PKP. The proliferation potential of conjunctival epithelium is relatively low, and this may partly explain the persistence of the epithelial defects. Oral mucosal epithelium is thought to be less well differentiated, and this may be an advantage in terms of short cell turnover time and a quicker wound-healing response after transplantation.[13,14] However, no comparison of the relative rates in epithelial healing for ocular surface epithelial cells compared with oral epithelial cells was attempted in this study. Hayashida and associates[20] used a rabbit model to demonstrate that in vivo and in cultivated sheets, p63- and integrin 1–positive cells manifested the higher proliferation characteristics of oral mucosal epithelial cells. Inatomi and associates[17] previously reported positive midterm results in patients who had undergone ocular surface reconstruction by COMET. This in vivo laser confocal microscopic study demonstrated that the stratified epithelium existed in the central zone of the two patients. The shape of apical cells and size and density of the basal cells were similar to normal cornea, suggesting the maintenance of a well-differentiated structure of graft after the ocular surface reconstruction. At present, it is unclear whether the epithelium examined in this study was transplanted allogenic corneal epithelium or regenerated epithelium derived from autologous cultivated oral mucosal epithelium on the peripheral cornea.

The results of experimental and clinical studies suggest that COMET is a promising and advantageous alternative to mucosal epithelium transplants for ocular surface reconstruction. This study documented the survival of ectopically transplanted oral mucosal epithelium and showed that the transplantation of autologous oral mucosal stem cells to donor corneal grafts avoids common epithelial complications. At present, the long-term survival of both

the transplanted oral mucosal epithelia and allogenic corneal grafts in this study continue to be monitored.

REFERENCES

1. Theng JTS, Tan DTH. Combined penetrating keratoplasty and limbal allograft transplantation for severe corneal burns. Ophthalmic Surg Lasers 1997;28:765–768.
2. Solomon A, Ellies P, Anderson DF, et al. Long-term outcome of keratoplimbal allograft with or without penetrating keratoplasty for total limbal stem cell deficiency. Ophthalmology 2002;109:1159–1166.
3. Pellegrini G, Traverso CE, Franzi AT, et al. Long-term restoration of damaged corneal surfaces with autologous cultivated corneal epithelium. Lancet 1997;349:990–993.
4. Tsai RJ, Li LM, Chen JK. Reconstruction of damaged corneas by transplantation of autologous limbal epithelial cells. N Engl J Med 2000;343:86–93.
5. Koizumi N, Inatomi T, Suzuki T, et al. Cultivated corneal epithelial stem cell transplantation in ocular surface disorders. Ophthalmology 2001;108:1569–1574.
6. Schwab IR, Reyes M, Isseroff RR. Successful transplantation of bioengineered tissue replacements in patients with ocular surface disease. Cornea 2000;19:421–426.
7. Ramaesh K, Dhillon B. Ex vivo expansion of corneal limbal epithelial/stem cells for corneal surface reconstruction. Eur J Ophthalmol 2003;13:515–524.
8. Meller D, Pires RT, Tseng SC. Ex vivo preservation and expansion of human limbal epithelial stem cells on amniotic membrane cultures. Br J Ophthalmol 2002;86:463–471.
9. Nakamura T, Inatomi T, Sotozono C, et al. Successful primary culture and autologous transplantation of corneal limbal epithelial cells from minimal biopsy for unilateral severe ocular surface disease. Acta Ophthalmol Scand 2004; 82:468–471.
10. Sangwan VS, Vemuganti GK, Iftekhar G, et al. Use of autologous cultured limbal and conjunctival epithelium in a patient with severe bilateral ocular surface disease induced by acid injury: a case report of unique application. Cornea 2003;22:478–481.
11. Tan DT, Ang LP, Beuerman RW. Reconstruction of the ocular surface by transplantation of a serum-free derived cultivated conjunctival epithelial equivalent. Transplantation 2004;77:1729–1734.
12. Nakamura T, Endo K, Cooper LJ, et al. The successful culture and autologous transplantation of rabbit oral mucosal epithelial cells on amniotic membrane. Invest Ophthalmol Vis Sci 2003;44:106–116.
13. Hata K, Kagami H, Ueda M, Torii S, Matsuyama M. The characteristics of cultured mucosal cell sheet as a material for grafting; comparison with cultured epidermal cell sheet. Ann Plast Surg 1995;34:530–538.
14. Ueda M, Hata K, Horie K, Torii S. The potential of oral mucosal cells for cultured epithelium: a preliminary report. Ann Plast Surg 1995;35:498–504.
15. Nakamura T, Inatomi T, Sotozono C, et al. Transplantation of cultivated autologous oral mucosal epithelial cells in patients with severe ocular surface disorders. Br J Ophthalmol 2004;88:1280–1284.
16. Nishida K, Yamamoto M, Hayashi Y, et al. Corneal reconstruction with tissue-engineered cell sheets composed of autologous oral mucosal epithelium. N Engl J Med 2004;351: 1187–1196.
17. Inatomi T, Nakamura T, Koizumi N, et al. Mid-term results on ocular surface reconstruction using cultivated autologous oral mucosal epithelial transplantation. Am J Ophthalmol 2006;141:267–275.
18. Eckard A, Stave J, Guthoff RF. In vivo investigations of the corneal epithelium with confocal Rostock laser scanning microscope (RLSM). Cornea 2006;25:127–131.
19. Tsubota K, Satake Y, Kaido M, et al. Treatment of severe ocular surface disorders with corneal epithelial stem-cell transplantation. N Engl J Med 1999;340:1697–1703.
20. Hayashida Y, Nishida K, Yamamoto M, et al. Ocular surface reconstruction using autologous rabbit oral mucosal epithelial sheets fabricated ex vivo on a temperature-responsive culture surface. Invest Ophthalmol Vis Sci 2005;46:1632–1639.

A carbohydrate-binding protein, Galectin-1, promotes proliferation of adult neural stem cells

Masanori Sakaguchi[a,b], Tetsuro Shingo[c], Takuya Shimazaki[a], Hirotaka James Okano[a], Mieko Shiwa[d], Satoru Ishibashi[e], Hideyuki Oguro[f], Mikiko Ninomiya[a,g,h], Toshihiko Kadoya[i], Hidenori Horie[i], Akira Shibuya[b], Hidehiro Mizusawa[e], Françoise Poirier[k], Hiromitsu Nakauchi[f], Kazunobu Sawamoto[a,h], and Hideyuki Okano[a,l]

[a]Department of Physiology and [h]Bridgestone Laboratory of Developmental and Regenerative Neurobiology, Keio University School of Medicine, Tokyo 160-8582, Japan; [b]Institute of Basic Medical Sciences, University of Tsukuba, Ibaraki 305-8575, Japan; [c]Department of Neurological Surgery, Okayama University Graduate School of Medicine and Dentistry, Okayama 700-8558, Japan; [d]Yokohama Laboratory, Ciphergen Biosystems KK, Kanagawa 204-0005, Japan; [e]Department of Neurology and Neurological Science, Graduate School of Medicine, Tokyo Medical and Dental University, Tokyo 113-8596, Japan; [f]Laboratory of Stem Cell Therapy, Center for Experimental Medicine, Institute of Medical Sciences, University of Tokyo, Tokyo 108-8639, Japan; [g]Department of Neurology, Saitama Medical School, Saitama 350-0495, Japan; [i]CMC R&D Laboratories, Pharmaceutical Division, Kirin Brewery, Gunma 370-0013, Japan; [j]Advanced Research Center for Biological Science, Waseda University, Tokyo 202-0021, Japan; and [k]Institut Jacques Monod, Unité Mixte de Recherche Centre National de la Recherche Scientifique 7592, Universities Paris 6 and Paris 7, Cedex 05 Paris, France

Edited by Fred H. Gage, The Salk Institute for Biological Studies, San Diego, CA and approved March 15, 2006 (received for review October 8, 2005)

In the subventricular zone of the adult mammalian forebrain, neural stem cells (NSCs) reside and proliferate to generate young neurons. We screened factors that promoted the proliferation of NSCs *in vitro* by a recently developed proteomics technique, the ProteinChip system. In this screen, we identified a soluble carbohydrate-binding protein, Galectin-1, as a candidate. We show herein that Galectin-1 is expressed in a subset of slowly dividing subventricular zone astrocytes, which includes the NSCs. Based on results from intraventricular infusion experiments and phenotypic analyses of knockout mice, we demonstrate that Galectin-1 is an endogenous factor that promotes the proliferation of NSCs in the adult brain.

lectin | mobilization | stem cell niche

Recently, neural stem cells (NSCs) residing in the adult CNS have been studied to elucidate the mechanisms of ongoing tissue maintenance (1) and to develop strategies for regenerating the damaged CNS (2, 3).

Two neurogenic regions have been identified in the forebrain (FB): the subventricular zone (SVZ) of the lateral ventricle (LV) (4–6) and the subgranular layer of the hippocampal dentate gyrus (7–9). NSCs in these regions can generate functional neurons in the adult brain (10–12). Clinically, soluble factors that regulate these progenitor cells may be useful for regenerating the damaged CNS (13). The identification of additional factors that promote the proliferation of stem cells will contribute to NSC biology and to the development of innovative strategies for brain repair.

The proliferation and differentiation of various adult stem cells are regulated by common soluble factors (14). OP9 is a cell line that has been used to screen for factors that support hematopoietic stem cells (HSCs) (15, 16). In the present study, we found that OP9 conditioned medium (CM) promoted neurosphere formation, by which the proliferation of NSCs can be monitored *in vitro* (17). Using the ProteinChip system (18), we identified Galectin-1 as one of the molecules responsible for this activity.

Galectin-1 is a soluble carbohydrate-binding protein (19, 20) that has been implicated in a variety of biological events (21, 22). Carbohydrates on the cell surface may be involved in the intercellular interactions of various stem cells, including NSCs (23–25) and HSCs (26). A recent report suggested that Galectin-1 promotes the proliferation of HSCs *in vitro* (27). However, its functions in NSCs remain unknown. Here, we report on the expression and function of Galectin-1 in the adult mammalian brain.

Results and Discussion

Galectin-1 Was Found in OP9CM. To examine how OP9 cells affect the proliferation of NSCs, we cultured neurosphere cells (17) with or without OP9CM. At a density of one cell per well, no neurospheres formed in cultures grown without OP9CM (Fig. 1*A*, Ctrl; $n = 800$ cells) (28). In contrast, at the same culture density, of the total cells grown with OP9CM ($n = 400$), 49 ($12.4 \pm 0.54\%$) initiated neurosphere formation (Fig. 1*A*, OP9). Interestingly, the CM from OP9 cells that were passaged repeatedly over 6 months (inactivated OP9, IA-OP9) did not support neurosphere formation (Fig. 1*A*, IA-OP9; $n > 800$).

To identify the OP9-derived molecules that enhanced neurosphere formation, we used an expression screen based on mass spectrometry (18) to detect molecules that were more abundant in OP9CM than in IA-OP9CM. A signal at ≈14.6 kDa showed a reproducible difference in peak height between the two CMs (Fig. 5, which is published as supporting information on the PNAS web site). This fraction was purified, concentrated, and separated by SDS/PAGE, and the band was cut from the gel and analyzed by tandem mass spectrometry (see *Materials and Methods*). We obtained two amino acid sequences (VRGEVASDAK and EDGTWGTEHR) that were identical to portions of the Galectin-1 protein ($n = 3$), suggesting that the 14.6-kDa peak was Galectin-1. Western blotting with a specific Ab showed that the OP9CM contained more Galectin-1 than did the IA-OP9CM ($n = 3$; $P < 0.01$).

Adding recombinant Galectin-1 protein (10 and 100 ng/ml) to the culture medium enhanced the formation of neurospheres cultured at 100 cells per well (Fig. 1*B*; $P < 0.01$, ANOVA). Galectin-1 did not mimic the full activity of the OP9CM, suggesting that there are other factors that enhance neurosphere formation in the OP9CM. The neurospheres grown with Galectin-1 (100 ng/ml) were larger (Fig. 6*A*, which is published as supporting information on the PNAS web site; $P < 0.05$), formed more secondary neurospheres (Fig. 6*B*; $P < 0.05$), and differentiated into neurons, astrocytes, and oligodendrocytes (Fig. 1*C*). Together, these results suggest that Galectin-1 is one of the factors in OP9CM that enhances neurosphere formation.

Expression of Galectin-1 in the Adult Mouse FB. To investigate the *in vivo* function of Galectin-1, we examined its expression in the

---

Conflict of interest statement: No conflicts declared.

This paper was submitted directly (Track II) to the PNAS office.

Freely available online through the PNAS open access option.

Abbreviations: SVZ, subventricular zone; LV, lateral ventricle; FB, forebrain; GFAP, glial fibrillary acidic protein; PCNA, proliferating cell nuclear antigen; NSC, neural stem cell; CM, conditioned medium; IA-OP9, inactivated OP9.

[l]To whom correspondence should be addressed at: Department of Physiology, Keio University School of Medicine, 35 Shinano-machi, Shinjuku-ku, Tokyo 160-8582, Japan. E-mail: hidokano@sc.itc.keio.ac.jp.

www.pnas.org/cgi/doi/10.1073/pnas.0508793103

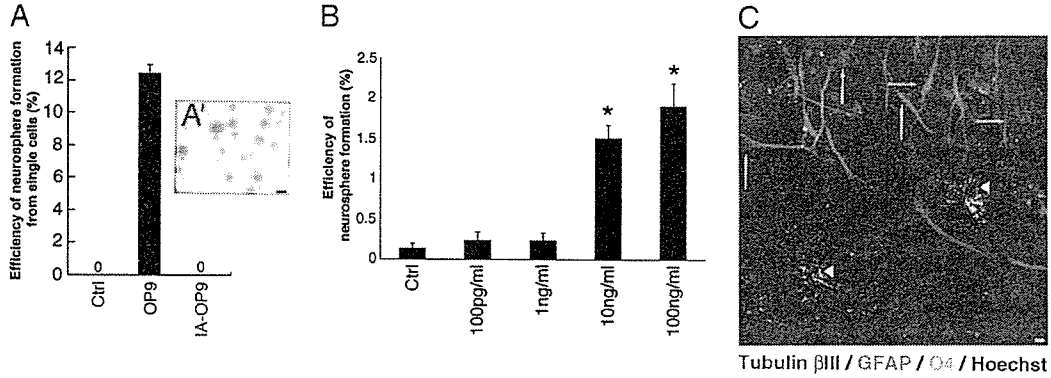

Fig. 1. Galectin-1 enhances neurosphere formation. (*A*) Effects of CM on neurosphere formation. Ctrl, control. (*A'*) The neurospheres initiated by OP9CM could be passaged more than five times. (*B*) Galectin-1 enhances neurosphere formation. Note that some neurospheres formed in the control cultures under this condition (culture density of 100 cells per well). *, $P < 0.01$. (*C*) The neurospheres initiated by Galectin-1 differentiated into neurons and glial cells. Representative images of differentiated cells from a neurosphere generated with recombinant Galectin-1 and immunostained with each neural lineage marker are shown. Tubulin βIII (neurons, red, white arrows), GFAP (astrocytes, green, green arrows), O4 (oligodendrocytes, light blue, arrowheads), and Hoechst (nucleus, dark blue) images were obtained by confocal laser microscopy. (Scale bars: *A*, 100 μm; *C*, 10 μm.)

mouse brain by using a Galectin-1-specific Ab (29). To confirm the specificity and sensitivity of the staining procedures, brain sections from a *galectin-1*-null mutant mouse (30) were simultaneously incubated with the same anti-Galectin-1 Ab, and we observed no staining (Fig. 7, which is published as supporting information on the PNAS web site).

In the adult mouse FB, as reported previously (31), subsets of neurons in the cortex were Galectin-1$^+$ (Fig. 7*A'*). In addition, we found Galectin-1 staining signals in the SVZ (Fig. 7*A''*) and dentate gyrus (Fig. 8*A*, which is published as supporting information on the PNAS web site), the two major adult neurogenic regions. RT-PCR analysis also showed that Galectin-1 is expressed in the SVZ (Fig. 8*B*). Almost all of the Galectin-1$^+$ cells in the adult SVZ expressed glial fibrillary acidic protein (GFAP) (Fig. 2*A*; see Fig. 8*C* for the confocal image), Nestin (Fig. 8*D*), and S100β (Fig. 8*E*). Some of these Galectin-1$^+$ cells were positive for Ki67 (Fig. 8*F*) (32), a nuclear marker of cellular replication. With regard to Galectin-1 expression in GFAP$^+$ cells outside the SVZ, we found that subsets of GFAP$^+$ cells in the subgranular layer and hilus were Galectin-1$^+$ (Fig. 8*A*), whereas most of the GFAP$^+$ cells in the cortex and striatum were Galectin-1$^-$ (Fig. 8 *G* and *H*). In the SVZ, the GFAP$^+$ astrocytes (type B cells) have been shown to act as NSCs (33, 34), which generate Dlx$^+$/Mash1$^+$ type C cells (35, 36) (Toida Kazunori, personal communication) and subsequently differentiate into PSA-NCAM$^+$/Dlx$^+$/Mash1$^-$ type A cells (in which PSA-NCAM is the polysialylated neural cell adhesion molecule) (35, 36). Among striatal neurons (Fig. 8*I*), Mash1$^+$ type C cells, and PSA-NCAM$^+$ type A cells (Fig. 8*J*), none showed Galectin-1 immunoreactivity. Dissociated SVZ cells were stained with

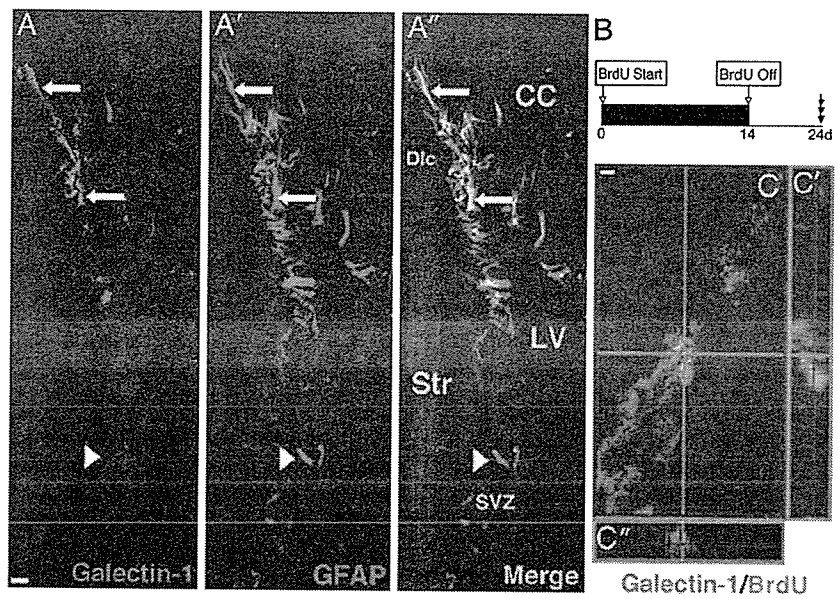

Fig. 2. Galectin-1 is detected in SVZ astrocytes. (*A*) Low-magnification images of Galectin-1 (*A*) and GFAP (*A'*) double immunostaining in the coronal section through the LV. Galectin-1 and GFAP double-positive cells are seen in the SVZ (arrows). Note there are some Galectin-1-negative cells among the GFAP$^+$ cells (e.g., arrowhead). (*A''*) Merged image. CC, corpus callosum; Str, striatum; Dlc, dorsolateral corner. (*B*) Experimental schema for marking slowly dividing cells. (*C*) Slowly dividing Galectin-1$^+$ cell. High-magnification confocal image of a Galectin-1 (green in cell soma) and BrdU (red in nucleus) double-positive cell in the SVZ. Sections were made after 2 weeks of oral BrdU administration followed by 10 days of wash-out. (*C'* and *C''*) 3D reconstruction images. (Scale bars: 5 μm.)

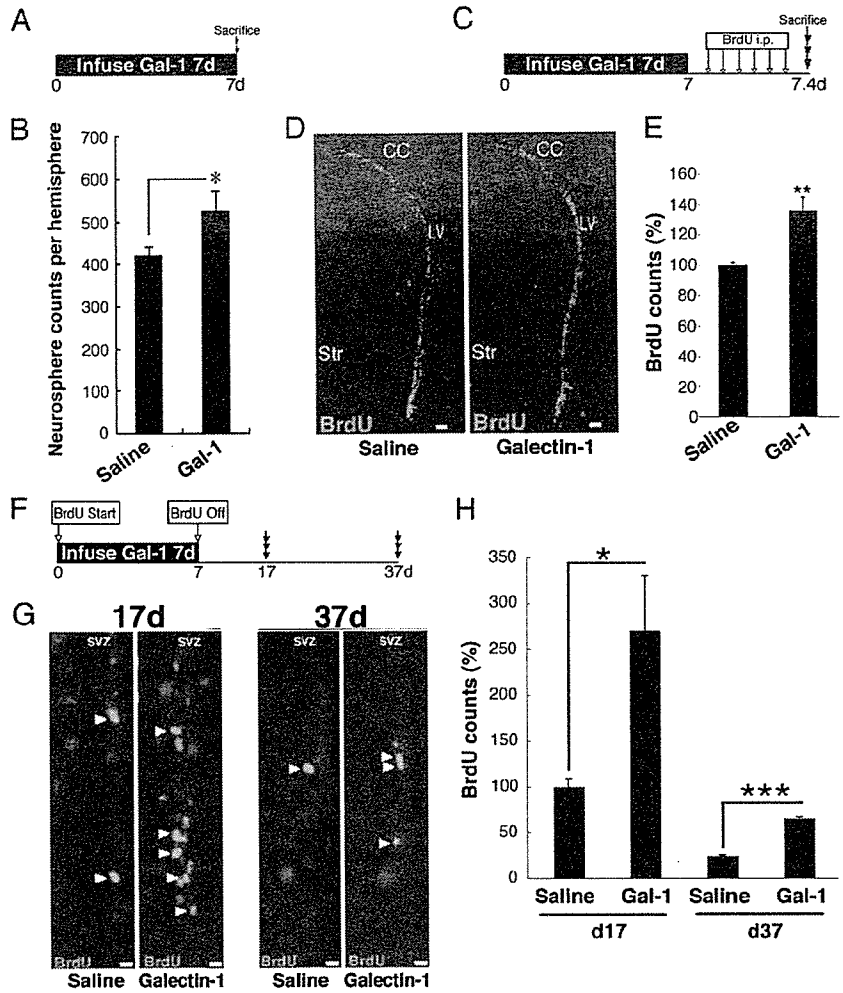

Fig. 3. Galectin-1 facilitates neural progenitor cell proliferation in the adult FB. (*A*) Experimental schema of the neurosphere formation assay after Galectin-1 infusion. (*B*) Galectin-1 significantly increased the number of neurosphere-initiating cells in the SVZ. *, $P < 0.05$. (*C*) Experimental schema of BrdU infusion after Galectin-1 infusion. (*D*) Low-magnification images of BrdU$^+$ cells in the SVZ after Galectin-1 infusion. (*E*) Galectin-1 infusion significantly increased the number of BrdU$^+$ cells in the SVZ. **, $P < 0.01$. (*F*) Experimental schema for labeling cells that retained BrdU long after Galectin-1 infusion. The mice were killed at the 17- or 37-day time point. (*G*) BrdU-labeled cells after infusion of saline or Galectin-1. (*H*) In the Galectin-1-infused brain, the number of BrdU$^+$ cells was significantly greater than in the saline-treated brain at 17 and 37 days. *, $P = 0.01$; ***, $P = 0.0006$. Str, striatum. (Scale bars: *D*, 50 μm; *G*, 15 μm.)

anti-Galectin-1 and anti-GFAP Abs to determine the percentages of each cell population in the SVZ. Of the total SVZ cells counted (n = 336 from three mice), 32.7 ± 6.38% (110 cells) were Galectin-1$^+$, and 31.3 ± 6.99% (105 cells) were GFAP$^+$. Of the GFAP$^+$ cells, 71.4 ± 1.48% were also Galectin-1$^+$. These results suggest that Galectin-1 is expressed in a subset of SVZ astrocytes.

To detect the slowly dividing NSC population in the SVZ (37), we gave BrdU to mice in their drinking water for 2 weeks and killed the mice 10 days later (Fig. 2*B*); this delay allowed the BrdU in the rapidly dividing type C cell population to be washed out and the type A cell population to migrate to a more rostral region, out of the SVZ (37). A subpopulation of the long-term BrdU-retaining cells expressed Galectin-1 (Fig. 2*C*). Thus, we conclude that Galectin-1 is expressed in a subset of GFAP$^+$ SVZ astrocytes that includes NSCs.

Galectin-1 Facilitates Proliferation of Neural Progenitor Cells in the Adult FB. The *in vitro* functions and *in vivo* expression pattern of Galectin-1 led us to examine whether it promotes adult neural progenitor proliferation *in vivo*. Galectin-1 protein was infused into the mouse LV for 7 days, and the number of neurospheres derived from the SVZ was counted (Fig. 3*A*); this number should reflect the number of progenitor cell types in the SVZ, including type B and C cells (36). As expected, significantly more neurospheres were formed by SVZ cells from the Galectin-1-infused adult brains than by SVZ cells from the control brains (Fig. 3*B*). The neurospheres in these cultures retained the properties of stem cells *in vitro*, and the proportion of neurons produced from the spheres was not significantly different (Galectin-1, 7.61 ± 0.61%; control, 5.84 ± 0.47%).

Next, we tested the effects of Galectin-1 on cell proliferation in the SVZ by infusing it into the LV, followed by BrdU injections every 2 h for 10 h (Fig. 3*C*). Thirty minutes after the last BrdU injection, the mice were killed. We counted the number of BrdU$^+$ cells in the SVZ of the LV and found a significant increase, on average, compared with the saline-infused control group (Fig. 3 *D* and *E*; $P < 0.01$; $n > 3$ mice each). There was no significant difference in the number of apoptotic cells in the SVZ between the two groups (Fig. 9 *A* and *B*, which is published as supporting information on the PNAS web site), suggesting that the Galectin-1-induced increase in BrdU$^+$ cells was caused by increased proliferation rather than increased cell survival.

Table 1. Galectin-1 increases the number of SVZ astrocytes in the adult brain

Treatment	No. of cells		
	Type B	Type C	Type A
Saline	40 ± 14	200 ± 12	64 ± 6.6
Galectin-1	66 ± 7.0*	280 ± 2.0*	64 ± 31
Galectin-1/saline relative ratio	1.7	1.4	1.0

Significantly increased numbers of SVZ astrocytes (type B cells) and type C cells were observed in the Galectin-1-infused brain. Data are the average counts from 50-μm sections. *, $P < 0.05$.

To determine what type of cells in the SVZ proliferated in response to the Galectin-1 infusion, we used cell-type markers (Fig. 10, which is published as supporting information on the PNAS web site) that allowed us to distinguish proliferating type B ($BrdU^+/Sox21^+/Dlx^-$), type C ($BrdU^+/Mash1^+$), and type A ($BrdU^+/Dlx^+/Mash1^-$) cells from others ($BrdU^+/Sox21^-$) (Table 1; see *Materials and Methods* for details). The Galectin-1 infusion significantly increased the number of proliferating type B and C cells (Table 1; $P < 0.05$, Mann–Whitney U test).

Infusion of Galectin-1 Protein Increases the Slowly Dividing SVZ Cells. We next examined the effect of Galectin-1 on the number of slowly dividing cells. We gave BrdU to mice in their drinking water during the 1-week infusion of Galectin-1 protein and killed them 17 or 37 days after the beginning of the infusion (Fig. 3*F*). There were significantly more $BrdU^+$ cells in the SVZ of the Galectin-1-infused brains than in that of the control brains at both time points (Fig. 3 *G* and *H*; day 17, $P = 0.01$, $n > 3$ each; day 37, $P < 0.001$, $n > 3$ each). These data suggest that Galectin-1 infusion increased the population of slowly dividing SVZ progenitor cells.

Galectin-1 exists in either a reduced or oxidized form, and only the reduced form possesses carbohydrate-binding activity (38). The infusion of CS-Galectin-1, a reduced form in which all of the cysteines responsible for its oxidation have been converted to serine (39), significantly increased the number of slowly dividing cells (Fig. 11, which is published as supporting information on the PNAS web site; day 17, $P < 0.001$, $n > 5$ mice each). In contrast, the oxidized Galectin-1 did not have a significant effect (Fig. 11*C*). These results suggest that the carbohydrate-binding capacity of the extracellularly administrated Galectin-1 is required for its effect on the number of slowly dividing cells. We also found that CS-Galectin-1 could bind to SVZ cells, including $GFAP^+$ astrocytes (unpublished data), suggesting that these cells are responsive to Galectin-1.

***Galectin-1*-Null Mice Have Fewer Neural Progenitor Cells in the Adult Brain.** To study the function of endogenous Galectin-1 in adult neural progenitor cells, we analyzed the phenotype of adult *galectin-1* mutant mice. First, we counted the number of cycling cells in the SVZ by using proliferating cell nuclear antigen (PCNA), a proliferation marker (40), and found significantly fewer in the *galectin-1*-null mice than in their wild-type littermates (Fig. 4 *A–C*; $P < 0.01$; $n > 3$ each). We also examined the number of type C cells by counting the $Mash1^+$ cells, of which there were also significantly fewer in the *galectin-1*-null mice than in wild-type littermates (Fig. 4 *D–F*; $P < 0.05$; $n > 3$ each). We then treated the animals with BrdU for 2 weeks, followed by a 10-day wash-out period (Fig. 4*G*), and found that there were significantly fewer slowly dividing cells in the SVZ of the *galectin-1*-null mice than in their wild-type littermates (Fig. 4 *H–J*; $P < 0.01$; $n > 3$ each). Furthermore, infusion of an

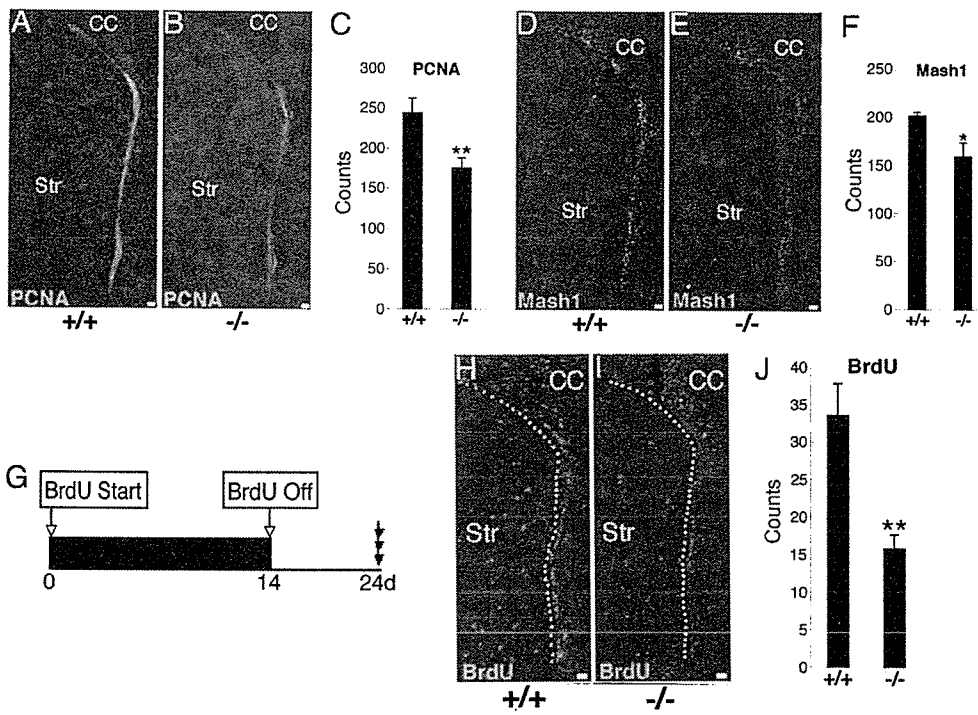

Fig. 4. Adult *galectin-1*-null mice show decreased neural progenitor cells. (*A–C*) Significantly fewer $PCNA^+$ cells were seen in the SVZ of *galectin-1*-null mice than in wild-type littermates. **, $P < 0.01$; $n > 3$ each. (*D–F*) Significantly fewer $Mash1^+$ type C cells were seen in the SVZ of *galectin-1* null mice than in wild-type littermates. *, $P < 0.05$; $n > 3$ each. (*G–J*) Fewer slowly dividing cells were seen in *galectin-1*-null mice than in wild-type mice. Slowly dividing cells in the SVZ were visualized as described in the legend of Fig. 2*B*. Dotted lines are drawn around the SVZ in *H* and *I*. (*J*) Significantly fewer long-term BrdU-retaining cells were observed in the SVZ of *galectin-1* mutant mice than in wild-type littermates. **, $P < 0.01$; $n > 3$ each. (Scale bars: 50 μm.)

anti-Galectin-1 neutralizing Ab (29) into the LV of adult wild-type mice significantly decreased the number of slowly dividing cells (Fig. 12, which is published as supporting information on the PNAS web site), a phenotype similar to that seen in *galectin-1*-null mutants (Fig. 4 *G–J*), suggesting that the endogenous Galectin-1 protein in the adult SVZ plays a role in the maintenance of neural progenitor cells. Moreover, the *galectin-1*-null mutation did not affect the number of apoptotic cells in the SVZ (Fig. 9 *C* and *D*). Together, these data suggest that Galectin-1 is required for the normal proliferation of type B and C cells in the adult brain.

The proliferation of adult and fetal NSCs is regulated by distinct mechanisms (41). Radial glial cells act as NSCs in the fetal and early postnatal brain and then may differentiate into astrocytes, expressing GFAP at approximately postnatal day (P) 7–15 (42, 43). Interestingly, Galectin-1 is not expressed before P9 in the FB (44). The brain of *galectin-1*-null mice at birth is indistinguishable from that of wild-type littermates (30, 45) except for an aberrant topography of olfactory axons (46). Therefore, Galectin-1 is most likely to play a role in adult NSCs rather than in embryonic NSCs. Taken together, our results demonstrate that Galectin-1 is expressed in slowly dividing SVZ astrocytes, which include the NSCs (34), and plays an important role in the proliferation of adult neural progenitor cells, including SVZ astrocytes. Stem cells reside in an area called a niche (47, 48), which has a characteristic cellular composition and signal mediators. In the niche, the state of each cell [i.e., cell cycle, apoptosis, and cell–cell or cell–extra cellular matrix (ECM) interactions] is strictly regulated to maintain stem cell homeostasis. Although ECM proteins are enriched in the SVZ (24, 49, 50), the niche for NSCs, the physiological significance of their carbohydrate structures has not been well characterized. In general, lectins exert their biological effects by binding to certain carbohydrate structures. Galectin-1's carbohydrate-binding ability is required for some functions but not others (27, 39, 51, 52). The present study suggests that the carbohydrate-binding activity of Galectin-1 is required for its promotion of adult neural progenitor cell proliferation. The analysis of Galectin-1 function will help us understand the important roles of carbohydrate molecules in stem cell biology, which may lead to the development of innovative therapies for human diseases.

Materials and Methods

Evaluation of OP9CM Activity. To assay the CM activity (see *Supporting Materials and Methods*, which is published as supporting information on the PNAS web site), neurospheres, prepared as described in ref. 53, were dissociated with trypsin and then FACS-sorted (*Supporting Materials and Methods*) at one cell per well directly into 96-well low-adhesion microtiter plates (Costar) containing each CM in a separate well. Human Galectin-1 was purchased from Genzyme Techne. To prepare the neurosphere CM (NSCM), neurospheres were cultured in the basal medium with 20 ng/ml human recombinant EGF (PeproTech, Rocky Hill, NJ) and FGF-2 (Genzyme Techne) for 48 h. To evaluate the activity of Galectin-1, the cells were sorted at 100 cells per well into NSCM-containing medium.

Molecular Identification of Galectin-1 in the CM. The OP9CM and IA-OP9CM preparations were analyzed by using the ProteinChip system (Ciphergen Biosystems). To screen the differences in peak heights, chemical surface chips that were positively charged, negatively charged, hydrophobic, C4, and Zn were used in the range of 500–200,000 Da. The affinity of the protein for each chip was monitored by using wash buffers of several pH values. To purify the 14.6-kDa protein, 200 ml of the OP9CM was freeze-dried, and a condensed solution was run on a Q-100 column (General Electric). The fraction that was eluted with 200 mM NaCl was used for SDS/PAGE. The 14.6-kDa band was cut from the gel and used for amino acid sequencing by tandem mass spectrometry.

Infusion into the SVZ and Adult Neurosphere Culture. Galectin-1 (2 or 14 μg), anti-Galectin-1 neutralizing Ab (rabbit IgG, 30 μg/ml, Kirin Brewery), or control rabbit IgG (30 μg/ml, Kirin Brewery) was dissolved in 0.9% saline with 1 mg/ml mouse serum albumin (Sigma) and infused into the LV as described in ref. 54 by using an osmotic pump (Alzet, Palo Alto, CA) at 0.5 μl/h for the given number of days. Adult neurosphere cultures from the infused brain samples were prepared as described in ref. 54.

Immunohistochemistry. Brains were perfusion-fixed with 4% paraformaldehyde (PFA) and postfixed in the same fixative overnight, and 50-μm sections were cut on a vibratome. Differentiated neurospheres grown on coverslips were immersion-fixed in 4% PFA for 15 min at room temperature. After three rinses in PBS, the neurospheres or sections were incubated for 1 h in TNB blocking solution (Vector Laboratories), incubated with primary antibodies overnight, and incubated for 60 min at room temperature with biotinylated secondary antibodies (1:200) or Alexa Fluor-conjugated secondary antibodies (1:200; Molecular Probes), unless otherwise noted. Biotinylated antibodies were visualized by using the Vectastain Elite ABC kit and TSA (Vector Laboratories). Anti-Galectin-1-neutralizing Abs were prepared as described in ref. 39. Other primary antibodies used in this study are described in *Supporting Materials and Methods*.

BrdU Labeling. For short-term labeling, after the intraventricular infusion of Galectin-1 for 7 days, mice received i.p. injections of BrdU (120 mg/kg dissolved in 0.007% NaOH in phosphate buffer; Sigma) every 2 h for 10 h and were killed 0.5 h after the last injection. For long-term labeling, 1 mg/ml BrdU was given to mice in their drinking water for 2 weeks (or 1 week in experiments involving the infusion of Galectin-1 or Abs). Mice were killed 10 or 30 days after the last day of infusion, and the brains were processed for immunohistochemistry.

Quantification of Histological Results. To quantify each cell type, 20 coronal vibratome sections of the SVZ (50 μm thick) were obtained at the level of the caudate-putamen (1.0–0 mm rostral to the bregma) from each hemisphere. The sections were stained for three different markers with BrdU (Sox21/BrdU, Dlx/BrdU, or Mash1/BrdU). Single confocal images were taken as 1-μm optical sections (LSM-510; Zeiss) from each vibratome section. The $BrdU^+$ nuclei that were positive for each marker (Sox21, Dlx, or Mash1) were counted, and the total number of $BrdU^+$ cells was multiplied by the ratio of the cells of each type to $BrdU^+$ cells, yielding the numbers for each cell type as follows: type B cells = total number of $BrdU^+$ [$(Sox21^+/BrdU^+)$ − $(Dlx^+/BrdU^+)$], type C cells = total number of $BrdU^+$ $(Mash1^+/BrdU^+)$, and type A cells = total number of $BrdU^+$ [$(Dlx^+/BrdU^+)$ − $(Mash1^+/BrdU^+)$]. The average number of each cell type per 50-μm section throughout the LV is indicated in each figure. Apoptotic cells were detected by using an ApoTag kit (Intergen, Purchase, NY). We quantified the cells in the LV contralateral to the infused side, because exposure to the increased concentration of reagent in the LV could have an artifactual effect.

Animals. For the adult mouse study, 8-week-old male mice were killed by anesthetic overdose. *galectin-1* knockout mice (129SJ background) are described in ref. 30. The animals were maintained on a 12-h light/12-h dark cycle with unlimited access to food and water. All experiments on live animals were performed in accordance with Keio University guidelines and regulations.

Statistical Analysis. Values are expressed as the mean ± SE. An unpaired *t* test (for two groups) or ANOVA with the Bonferroni correction (for more than three groups) was used to evaluate the differences of the averages, unless otherwise noted.

We thank K. Sakurada, S. Kaneko, Masatake Osawa, H. Miyoshi, K. Nakashima, T. Imai, and S. Yamanaka for critical advice; T. Nakano (Osaka University, Japan), T. Kitamura (University of Tokyo), T. Seki (Juntendo University, Tokyo), H. Ohba (Keio University), K. Adachi (Keio University), O. Yamada (Keio University), and G. Panganiban (University of Wisconsin, Madison) for experimental materials; R. Wakatabe, Y. Fukase, Mitsujiro Osawa, Y. Morita, T. Yamashita, K. Sango, S. Kuno, Y. Hayakawa, and Y. Fujita for technical assistance; M. Ito, K. Inoue, and A. Hirayama for secretarial assistance; and S. Sakaguchi for critical advice and continuous support. This work was supported by grants from the Ministry of Education, Culture, Sports, Science, and Technology of Japan (MEXT); Core Research for Evolutional Science and Technology of the Japan Society and Technology Agency (to H. Okano); the 21st Century Centers of Excellence Program of MEXT (to Keio University and Tokyo Medical and Dental University); Association pour la Recherche sur le Cancer, Ligue Nationale Française Contre le Cancer, and Association Française Contre les Myopathies (to F.P.); and the National Institutes of Health and National Institute of Neurological Disorders and Stroke (to M. Sakaguchi).

1. Alvarez-Buylla, A. & Lim, D. A. (2004) *Neuron* **41**, 683–686.
2. Okano, H. (2002) *J. Neurosci. Res.* **69**, 698–707.
3. Lie, D. C., Song, H., Colamarino, S. A., Ming, G. L. & Gage, F. H. (2004) *Annu. Rev. Pharmacol. Toxicol.* **44**, 399–421.
4. Lois, C. & Alvarez-Buylla, A. (1993) *Proc. Natl. Acad. Sci. USA* **90**, 2074–2077.
5. Levison, S. W. & Goldman, J. E. (1993) *Neuron* **10**, 201–212.
6. Luskin, M. B. (1993) *Neuron* **11**, 173–189.
7. Altman, J. & Das, G. D. (1965) *J. Comp. Neurol.* **124**, 319–335.
8. Bayer, S. A., Yackel, J. W. & Puri, P. S. (1982) *Science* **216**, 890–892.
9. Eriksson, P. S., Perfilieva, E., Bjork-Eriksson, T., Alborn, A. M., Nordborg, C., Peterson, D. A. & Gage, F. H. (1998) *Nat. Med.* **4**, 1313–1317.
10. van Praag, H., Schinder, A. F., Christie, B. R., Toni, N., Palmer, T. D. & Gage, F. H. (2002) *Nature* **415**, 1030–1034.
11. Carleton, A., Petreanu, L. T., Lansford, R., Alvarez-Buylla, A. & Lledo, P. M. (2003) *Nat. Neurosci.* **6**, 507–518.
12. Gheusi, G., Cremer, H., McLean, H., Chazal, G., Vincent, J. D. & Lledo, P. M. (2000) *Proc. Natl. Acad. Sci. USA* **97**, 1823–1828.
13. Nakatomi, H., Kuriu, T., Okabe, S., Yamamoto, S., Hatano, O., Kawahara, N., Tamura, A., Kirino, T. & Nakafuku, M. (2002) *Cell* **110**, 429–441.
14. Reya, T., Morrison, S. J., Clarke, M. F. & Weissman, I. L. (2001) *Nature* **414**, 105–111.
15. Takakura, N., Kodama, H. & Nishikawa, S. (1996) *J. Exp. Med.* **184**, 2301–2309.
16. Ueno, H., Sakita-Ishikawa, M., Morikawa, Y., Nakano, T., Kitamura, T. & Saito, M. (2003) *Nat. Immunol.* **4**, 457–463.
17. Reynolds, B. A. & Weiss, S. (1992) *Science* **255**, 1707–1710.
18. Fung, E. T., Thulasiraman, V., Weinberger, S. R. & Dalmasso, E. A. (2001) *Curr. Opin. Biotechnol.* **12**, 65–69.
19. Teichberg, V. I., Silman, I., Beitsch, D. D. & Resheff, G. (1975) *Proc. Natl. Acad. Sci. USA* **72**, 1383–1387.
20. Barondes, S. H., Castronovo, V., Cooper, D. N., Cummings, R. D., Drickamer, K., Feizi, T., Gitt, M. A., Hirabayashi, J., Hughes, C., Kasai, K., *et al.* (1994) *Cell* **76**, 597–598.
21. Perillo, N. L., Marcus, M. E. & Baum, L. G. (1998) *J. Mol. Med.* **76**, 402–412.
22. Leffler, H. (2001) *Results Probl. Cell Differ.* **33**, 57–83.
23. Capela, A. & Temple, S. (2002) *Neuron* **35**, 865–875.
24. Mercier, F., Kitasako, J. T. & Hatton, G. I. (2002) *J. Comp. Neurol.* **451**, 170–188.
25. Yanagisawa, M., Liour, S. S. & Yu, R. K. (2004) *J. Neurochem.* **91**, 804–812.
26. Pipia, G. G. & Long, M. W. (1997) *Nat. Biotechnol.* **15**, 1007–1011.
27. Vas, V., Fajka-Boja, R., Ion, G., Dudics, V., Monostori, E. & Uher, F. (2005) *Stem Cells* **23**, 279–287.
28. Tropepe, V., Sibilia, M., Ciruna, B. G., Rossant, J., Wagner, E. F. & van der Kooy, D. (1999) *Dev. Biol.* **208**, 166–188.
29. Horie, H., Inagaki, Y., Sohma, Y., Nozawa, R., Okawa, K., Hasegawa, M., Muramatsu, N., Kawano, H., Horie, M., Koyama, H., *et al.* (1999) *J. Neurosci.* **19**, 9964–9974.
30. Poirier, F. & Robertson, E. J. (1993) *Development (Cambridge, U.K.)* **119**, 1229–1236.
31. Joubert, R., Kuchler, S., Zanetta, J. P., Bladier, D., Avellana-Adalid, V., Caron, M., Doinel, C. & Vincendon, G. (1989) *Dev. Neurosci.* **11**, 397–413.
32. Brown, D. C. & Gatter, K. C. (1990) *Histopathology* **17**, 489–503.
33. Seri, B., Garcia-Verdugo, J. M., McEwen, B. S. & Alvarez-Buylla, A. (2001) *J. Neurosci.* **21**, 7153–7160.
34. Doetsch, F., Caille, I., Lim, D. A., Garcia-Verdugo, J. M. & Alvarez-Buylla, A. (1999) *Cell* **97**, 703–716.
35. Parras, C. M., Galli, R., Britz, O., Soares, S., Galichet, C., Battiste, J., Johnson, J. E., Nakafuku, M., Vescovi, A. & Guillemot, F. (2004) *Embo. J.* **23**, 4495–4505.
36. Doetsch, F., Petreanu, L., Caille, I., Garcia-Verdugo, J. M. & Alvarez-Buylla, A. (2002) *Neuron* **36**, 1021–1034.
37. Morshead, C. M., Reynolds, B. A., Craig, C. G., McBurney, M. W., Staines, W. A., Morassutti, D., Weiss, S. & van der Kooy, D. (1994) *Neuron* **13**, 1071–1082.
38. Whitney, P. L., Powell, J. T. & Sanford, G. L. (1986) *Biochem. J.* **238**, 683–689.
39. Inagaki, Y., Sohma, Y., Horie, H., Nozawa, R. & Kadoya, T. (2000) *Eur. J. Biochem.* **267**, 2955–2964.
40. Yu, C. C. & Filipe, M. I. (1993) *Histochem. J.* **25**, 843–853.
41. Shi, Y., Chichung Lie, D., Taupin, P., Nakashima, K., Ray, J., Yu, R. T., Gage, F. H. & Evans, R. M. (2004) *Nature* **427**, 78–83.
42. Tramontin, A. D., Garcia-Verdugo, J. M., Lim, D. A. & Alvarez-Buylla, A. (2003) *Cereb. Cortex* **13**, 580–587.
43. Alvarez-Buylla, A., Garcia-Verdugo, J. M. & Tramontin, A. D. (2001) *Nat. Rev. Neurosci.* **2**, 287–293.
44. Poirier, F., Timmons, P. M., Chan, C. T., Guenet, J. L. & Rigby, P. W. (1992) *Development (Cambridge, U.K.)* **115**, 143–155.
45. Colnot, C., Fowlis, D., Ripoche, M. A., Bouchaert, I. & Poirier, F. (1998) *Dev. Dyn.* **211**, 306–313.
46. Puche, A. C., Poirier, F., Hair, M., Bartlett, P. F. & Key, B. (1996) *Dev. Biol.* **179**, 274–287.
47. Schofield, R. (1978) *Blood Cells* **4**, 7–25.
48. Spradling, A., Drummond-Barbosa, D. & Kai, T. (2001) *Nature* **414**, 98–104.
49. Campos, L. S., Leone, D. P., Relvas, J. B., Brakebusch, C., Fassler, R., Suter, U. & Ffrench-Constant, C. (2004) *Development (Cambridge, U.K.)* **131**, 3433–3444.
50. Emsley, J. G. & Hagg, T. (2003) *Exp. Neurol.* **183**, 273–285.
51. Liu, F. T. & Rabinovich, G. A. (2005) *Nat. Rev. Cancer* **5**, 29–41.
52. Wells, V. & Mallucci, L. (1991) *Cell* **64**, 91–97.
53. Shimazaki, T., Shingo, T. & Weiss, S. (2001) *J. Neurosci.* **21**, 7642–7653.
54. Shingo, T., Gregg, C., Enwere, E., Fujikawa, H., Hassam, R., Geary, C., Cross, J. C. & Weiss, S. (2003) *Science* **299**, 117–120.

Circulation
JOURNAL OF THE AMERICAN HEART ASSOCIATION

American Heart Association®
Learn and Live℠

Transfection of Human Hepatocyte Growth Factor Gene Ameliorates Secondary Lymphedema via Promotion of Lymphangiogenesis

Yukihiro Saito, Hironori Nakagami, Ryuichi Morishita, Yoichi Takami, Yasushi Kikuchi, Hiroki Hayashi, Tomoyuki Nishikawa, Katsuto Tamai, Nobuyoshi Azuma, Tadahiro Sasajima and Yasufumi Kaneda

Circulation 2006;114;1177-1184; originally published online Sep 4, 2006;
DOI: 10.1161/CIRCULATIONAHA.105.602953
Circulation is published by the American Heart Association. 7272 Greenville Avenue, Dallas, TX 72514
 Print ISSN: 0009-7322. Online ISSN: 1524-4539

Transfection of Human Hepatocyte Growth Factor Gene Ameliorates Secondary Lymphedema via Promotion of Lymphangiogenesis

Yukihiro Saito, MD; Hironori Nakagami, MD, PhD; Ryuichi Morishita, MD, PhD; Yoichi Takami, MD; Yasushi Kikuchi, MD, PhD; Hiroki Hayashi, BS; Tomoyuki Nishikawa, PhD; Katsuto Tamai, MD, PhD; Nobuyoshi Azuma, MD, PhD; Tadahiro Sasajima, MD, PhD; Yasufumi Kaneda, MD, PhD

Background—Lymphedema is a disorder of the lymphatic vascular system characterized by impaired lymphatic return and swelling of the extremities. Treatment for this disabling condition remains limited and largely ineffective. The goal of the present study was to investigate the therapeutic efficacy of hepatocyte growth factor (HGF) in animal models of lymphedema.

Methods and Results—Immunofluorescent analysis demonstrated that canine primary lymphatic endothelial cells (cLECs) were positive for lymphatic-specific markers (vascular endothelial growth factor receptor-3, LYVE-1, podoplanin, and Prox1) and the HGF receptor c-Met. Treating cLECs with human recombinant HGF resulted in a dose-dependent increase in cell growth and migration and increased activity of extracellular signal-regulated kinase and Akt. In human LECs, c-Met also was expressed, and treatment with HGF increased cell growth and migration in a dose-dependent manner. Transfection of human HGF plasmid DNA in cLECs also increased the c-*fos* promoter activity. Furthermore, weekly HGF gene transfer in a rat tail lymphedema model by disruption of lymphatic vessels resulted in a decrease in lymphedema thickness. Although expression of the endothelial cell marker PECAM-1 was increased in both HGF- and vascular endothelial growth factor 165–injected groups, expression of LEC markers (LYVE-1 and Prox1) was increased only in the HGF-injected group.

Conclusions—These data demonstrate that expression of HGF via plasmid transfer improves lymphedema via promotion of lymphangiogenesis. Further studies to determine the clinical utility of this approach would be of benefit to patients with lymphedema. (***Circulation*. 2006;114:1177-1184.**)

Key Words: gene therapy ■ hepatocyte growth factor ■ lymphangiogenesis

The lymphatic vascular system maintains tissue fluid homeostasis and plays a role in the afferent immune response.[1,2] Anatomic or functional obstruction in the lymphatic system after radical surgery or radiotherapy[3,4] can result in the progressive accumulation of protein-rich fluid in the interstitial spaces (lymphedema). Despite substantial advances in surgical and conservative techniques, therapeutic options for management of lymphedema are limited.[4,5]

Clinical Perspective p 1184

Recent studies suggest that lymphangiogenesis that can be stimulated by various cytokines.[6,7] For example, vascular endothelial growth factor (VEGF)-C and -D promote lymphangiogenesis by activating the VEGF receptor-3 (VEGFR-3), which is expressed on lymphatic endothelial cells (LECs).[8] Furthermore, VEGF-C–deficient mice fail to develop a functional lymphatic system,[9] transgenic expression of soluble VEGFR-3 results in pronounced lymphedema,[10] and gene transfer of VEGF-C effectively reduces lymphedema in an animal model.[11] Another study reported that angiopoietin-1 also promotes lymphatic vessel formation through Tie2.[12]

Hepatocyte growth factor (HGF) is a mesenchyme-derived pleiotropic factor that regulates growth, motility, and morphogenesis of various types of cells and thus is considered a humoral mediator of the epithelial-mesenchymal interactions responsible for morphogenic tissue interactions during embryonic development and organogenesis.[13,14] Moreover, the presence of a local HGF system (HGF and its specific receptor, c-Met) has been characterized in vascular cells in vitro and in vivo.[15] Our group and others have demonstrated that HGF treatment results in an increase in aortic endothelial

Received November 22, 2005; revision received June 19, 2006; accepted July 14, 2006.

From the Divisions of Gene Therapy Science (Y.S., H.N., Y.T., Y.K., H.H., T.N., K.T., Y.K.) and Clinical Gene Therapy (R.M.), Graduate School of Medicine, Osaka University, Osaka, and Department of Surgery, Asahikawa Medical University, Hokkaido (Y.S., N.A., T.S.), Japan.

Correspondence to Hironori Nakagami, MD, PhD, Assistant Professor, Division of Gene Therapy Science, Graduate School of Medicine, Osaka University, 2-2 Yamadaoka, Suita, Osaka 565-0871, Japan. E-mail nakagami@gts.med.osaka-u.ac.jp

Circulation is available at http://www.circulationaha.org

DOI: 10.1161/CIRCULATIONAHA.105.602953

cell proliferation and migration and that intramuscular injection of "naked" human HGF plasmid resulted in a significant increase in blood flow and capillary density in a rat and rabbit ischemic model.[16,17] Furthermore, a recent study reported that c-Met was highly expressed in LECs and that HGF was a strong promoter of lymphatic vessel formation.[18] Therefore, the goal of the present study was to investigate the therapeutic efficacy of HGF in animal models of lymphedema.

Methods

Cell Culture

Canine LECs (cLECs), canine aortic endothelial cells (cAECs), and canine venous endothelial cells (cVECs) isolated from canine thoracic ducts, aorta, or vein were cultured as previously described with some modifications.[19] Briefly, adult mongrel female dogs (8.0 to 10.0 kg body weight; Nihon Nosan Inc, Yokohama, Japan) were anesthetized with thiamylal sodium (50 mg/kg IV) and then intubated. For visualization of the thoracic duct, 20 mL IP of 0.5% patent blue was injected. Ten to 15 cm of the thoracic duct, aorta, or vein was isolated and placed in Hanks' buffered salt solution at 4°C and then skeletonized rapidly. Vessels were flushed with cold Hanks' buffered salt solution and incubated with collagenase solution (500 U/mL in Hanks' buffered salt solution, Worthington Biochemical Co, Lakewood, NJ) for 10 minutes at 37°C. Cells were harvested by washing vessels and subsequent centrifugation, and cells were maintained in endothelial basal medium supplemented with 20% FBS and endothelial growth supplement on 0.1% gelatin-coated culture dishes. Cultures were incubated at 37°C in a humidified atmosphere of 95% air/5% CO_2 with exchange of medium every 2 days. These cells were further purified with magnetic microbeads (Miltenyi Biotech, Bergisch Gladbach, Germany) attached to an anti–von Willebrand factor or an anti–LYVE-1 antibody as previously described[20] with slight modifications. These cells were used at passages 5 to 8 for subsequent experimental protocols.

Human LECs were from AngioBio Co (Del Mar, Calif) and were used at passages 5 to 8 for subsequent experimental protocols.

Immunofluorescent Analysis

Cells on glass coverslips and 8-μm cryostat sections of rat tail tissue were fixed in 4% paraformaldehyde or ethanol for 10 minutes. The samples were permeabilized with 0.2% Triton X-100 in phosphate-buffered saline (PBS) for 5 minutes. After blocking in 5% skim milk, the samples were stained with primary antibodies, including polyclonal rabbit anti-human von Willebrand factor (Dako, Glostrup, Denmark), polyclonal goat anti-human PECAM-1 (Santa Cruz Biotechnology, Inc, Santa Cruz, Calif), polyclonal rabbit anti-human VEGFR-3 (CHEMICON, Temecula, Calif), LYVE-1, podoplanin, Prox1 (Research Diagnostics, Inc, Flanders, NJ), or polyclonal rabbit anti–c-Met (Santa Cruz Biotechnology, Inc) for 1 hour at room temperature. Corresponding secondary antibodies were labeled with AlexaFluor488 or AlexaFluor546 (Molecular Probes, Eugene, Ore).

MTS Assay and c-*fos* Promoter Assay

Cell proliferation of LECs or endothelial cells seeded in 6-well plates was measured with the MTS [3-(4,5-dimethylthiazol-2-yl)-5-(3-carboxymethoxyphenyl)-2-(4-sulfophenyl)-2H- tetrazolium] assay at 48 hours after treatment with recombinant HGF (a kind gift from K. Matsumoto, Osaka University, Osaka, Japan), as previously described.[21] Approximately 100 μL CellTiter 96 One Solution Reagent (Promega, Madison, Wis) in 500 μL of Dulbecco's modified Eagle's medium was added to each well, and absorbance was measured at 490 nm. The c-*fos* promoter assay was performed in cLECs by cotransfection with the c-*fos*–luciferase reporter gene (p2FTL) using Lipofectamine2000 Transfection Regent (Invitrogen, Carlsbad, Calif). The c-*fos*–luciferase reporter gene consisted of 2 copies of the c-*fos* 5′-regulated enhancer element (−357 to −276), the herpes simplex virus thymidine kinase gene promoter (−200 to 70), and the luciferase gene. At 1 hour after transfection, transfected cells were incubated with serum-free medium for 24 hours. Cells were washed with PBS and lysed for 15 minutes with 200 μL cell lysis buffer at room temperature. Then, 20 μL cell extract was mixed with 100 μL luciferase assay reagent, and the light produced was measured for 30 seconds with a luminometer.

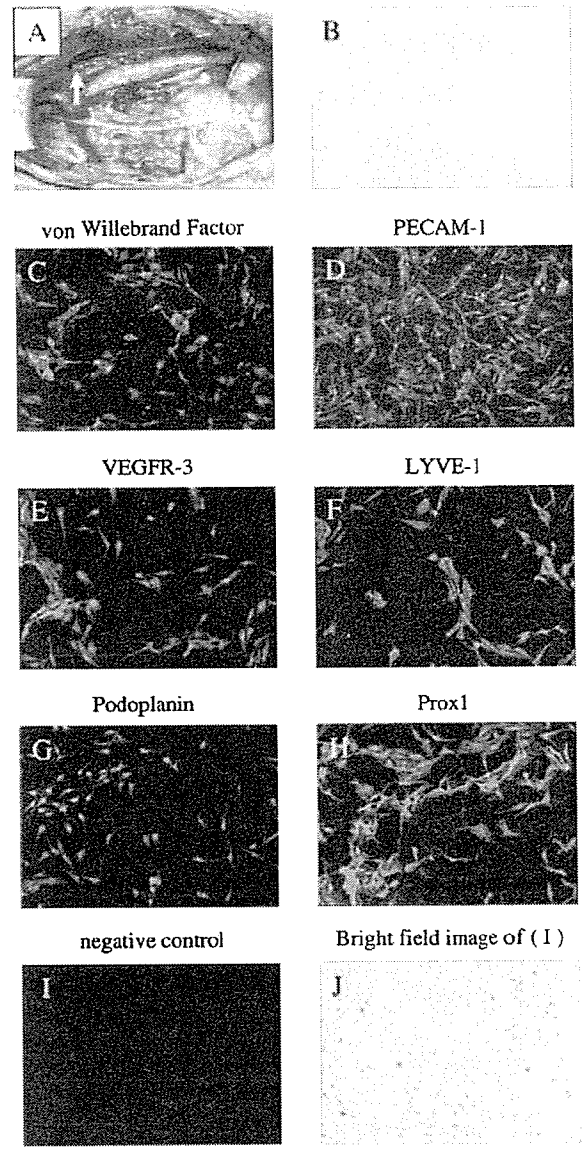

Figure 1. LEC culture. A, Canine thoracic ducts stained with patent blue (arrow). For visualization, 0.5% patent blue was injected intraperitoneally. B, Representative image of cultured cells obtained from canine thoracic ducts by injection of collagenase showing a monolayer with a uniform cobblestone appearance (×40 magnification). C–H, Representative pictures of immunofluorescent stains for the endothelial cell markers von Willebrand factor (C) and PECAM-1 (D) and for the LEC markers VEGFR-3 (E), LYVE-1 (F), podoplanin (G), and Prox1 (H) (×100 magnification).

Cell Migration

Migration of LECs was estimated in a modified Boyden chamber as previously described.[22] In brief, polyvinylpyrrolidone-free polycarbonate membranes (Neuro Probe Inc, Gaithersburg, Md) with 8-μm pores were coated with 0.1% gelatin overnight and then washed with PBS to remove excess coating. Next, 28 μL Dulbecco's modified

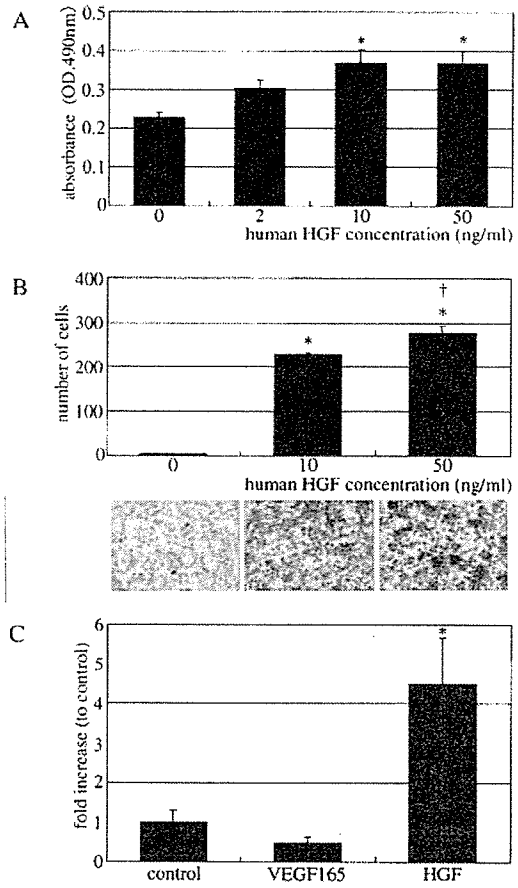

Figure 2. HGF promotes LEC proliferation and migration. A, B, Effect of recombinant HGF on cLECs as demonstrated by the MTS and migration assay. Middle, Typical images of each group (×200 magnification). n=9. *P<0.05 vs HGF 0 ng/mL; †P<0.05 vs HGF 10 ng/mL. C, Effect of HGF plasmid on c-*fos* promoter activity in LEC. n=4. *P<0.05 vs control, VEGF165.

Eagle's medium with or without recombinant HGF (10 or 50 ng/mL) was placed in the lower chamber. The membrane was positioned above the lower chamber, and 10^6 cells/mL were suspended in 50 μL Dulbecco's modified Eagle's medium with or without recombinant HGF (10 or 50 ng/mL) and then added to the upper chamber. The Boyden chamber was incubated at 37°C for 4 hours. After incubation, the membrane was removed, and the cells on the upper side of the membrane were scraped off. The cells on the lower side of the membrane were stained with Diff-Quick (Sysmex, Hyogo, Japan), and the cells were counted in 5 randomly chosen fields under ×200 magnification.

Western Blotting

Western blotting was performed for analysis of extracellular signal-regulated kinase (ERK) and Akt expression using a phospho-specific antibody as previously described.[23] After treatment, cells were extracted with a lysis buffer (50 mmol/L Tris(hydroxymethyl)methylomine-chloride, 2.5 mmol/L ethyleneglycoltetraacetic acid, 1 mmol/L ethylenediaminetetraacetic acid, 10 mmol/L sodium fluorescein, 1% Triton X-100, 1 mmol/L phenylmethylsulfonyl fluoride, 2 mmol/L Na_3VO_4). Samples containing 20 μg protein were separated on 10% SDS polyacrylamide gels, transferred to nitrocellulose membranes (Hybond ECL, Amersham), and incubated with a polyclonal antibody against phosphospecific or total ERK (polyclonal rabbit immunoglobulin G [IgG], 1:1000, Cell Signaling Technology, Beverly, Mass) or phosphospecific or total Akt (polyclonal rabbit IgG, 1:1000, Cell Signaling Technology) at 4°C overnight. The

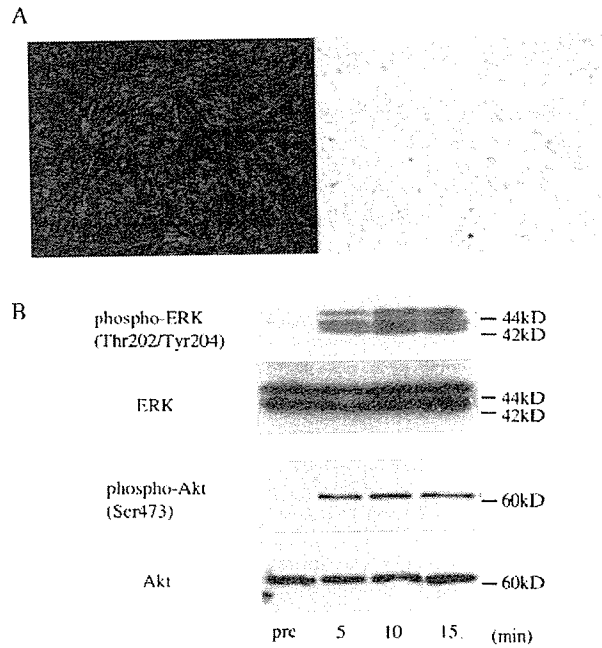

Figure 3. HGF signaling in LECs. A, Representative image of immunofluorescent stains for c-Met in cLECs (×100 magnification). B, Typical Western blot of ERK or Akt and phosphorylated ERK or Akt in cLECs before and 5, 10, and 15 minutes after treatment with human recombinant HGF (50 ng/mL).

membranes were then washed and incubated with a 1:2000 dilution of anti-rabbit IgG horseradish peroxidase–conjugated antibody (Amersham). Bound antibodies were detected by enhanced chemiluminescence (Amersham) and Hyperfilm-MP (Amersham).

Inhibition of ERK and Akt

cLECs were pretreated with a mitogen-activated protein kinase kinase (MEK) inhibitor, U0126 (50 μmol/L; Calbiochem, San Diego, Calif) or PD98059 (30 μmol/L; Calbiochem), and an inhibitor of phosphatidylinositol 3-kinase (PI3K), LY294002 (50 μmol/L; Calbiochem) or wortmannin (100 nmol/L; Calbiochem) for 1 hour. Then, the cells were treated by the inhibitors and recombinant HGF (50 ng/mL) for 24 hours in preparation for assays.

Gene Transfer Protocol in a Rat Tail Model

A rat lymphedema model was created as previously described[24] with slight modification. Briefly, an 8-week-old male Sprague-Dawley rat (Oriental Bio Science Co, Ltd, Kyoto, Japan) was anesthetized with pentobarbital sodium (50 mg/kg IP), and 0.2 mL of 0.5% patent blue was injected into the tip of the tail for visualization of lymphatic vessels. At the base of the tail, a circumferential incision was made through the dermis to sever the superficial lymphatic network. The blue lymphatic vessels were ligated with 6-0 silk suture or cauterized. Cauterization was applied to the edges of the circumferential wound, which resulted in a 2- to 4-mm gap between the skin edges, followed by secondary healing at the site of ligation.

In total, 60 rats were randomly assigned to 1 of 6 groups: human HGF plasmid (200 μg/0.1 mL; inserted into pVAX),[25] human VEGF165 plasmid (200 μg/0.1 mL; inserted into pCAGGS),[25] green fluorescent protein (GFP) plasmid (200 μg/0.1 mL), saline, operation only, and no operation (n=10 in each group). HGF, VEGF165, GFP plasmid, or 0.1 mL saline was injected intramuscularly at the distal operated site with a 30-gauge needle on days 1, 7, and 14 after surgery. Lymphatic vessel quantification was performed by assessing positive immunofluorescent staining for anti-PECAM-1, LYVE-1, Prox1, and c-Met in 5 randomly selected fields as previously described.[11]